SOLVING THREE DIMENSIONAL MAXWELL EIGENVALUE PROBLEMS WITH FOURTEEN BRAVAIS LATTICES*

TSUNG-MING HUANG†, TIEXIANG LI‡, WEI-DE LI§, JIA-WEI LIN¶, WEN-WEI LIN ¶, AND HENG TIAN ¶

Abstract. Calculation of band structures of three dimensional photonic crystals amounts to solving large-scale Maxwell eigenvalue problems, which are notoriously challenging due to high multiplicity of zero eigenvalues. In this paper, we try to address this problem in such a broad context that band structures of three dimensional isotropic photonic crystals in all 14 Bravais lattices can be efficiently computed in a unified framework. In this work, we uncover the delicate machinery behind several key results of our framework and on the basis of this new understanding we drastically simplify the derivations, proofs and arguments. Particular effort is made on reformulating the Bloch condition for all 14 Bravais lattices in the redefined orthogonal coordinate system, and establishing eigen-decomposition of discrete partial derivative operators by identifying the hierarchical structure of the underlying normal (block) companion matrix, and reducing the eigen-decomposition of the double-curl operator to a simple factorization of a 3-by-3 complex skew-symmetric matrix. With the validity of the novel nullspace free method in the broad context, we perform some calculations on one benchmark system to demonstrate the accuracy and efficiency of our algorithm to solve Maxwell eigenvalue problems.

Key words. Maxwell Eigenvalue Problems, three-dimensional photonic crystals, Bravais lattices, nullspace free method, FAME

AMS subject classifications. 15A18, 15A90, 65F15

1. Introduction.

The photonic crystal (PC) is an essential device when light is manipulated in optoelectronics industry. A PC is a one-, two- or three-dimensional (1D, 2D, 3D) periodic structure which is composed of different optical media that can purposefully affect the electromagnetic wave propagation. This term is coined after Yablonovitch [40] and John [26]'s milestone work in 1987. In recent years, the research about PC is booming due to the emergence of topological PCs (or photonic topological insulators) [34], especially the 3D topological PCs. To determine whether a PC is the topological PC, the calculation of band structures is indispensable [29]. To practically know the band structure of a 3D isotropic/anisotropic PC, we need to first recast the source-free Maxwell's equations in frequency domain [38] as follows, with a specific medium whose intrinsic properties are described by a 3-by-3 permeability matrix μ and a permittivity matrix ε, respectively,

$$\nabla \times \boldsymbol{E} = \imath\omega\mu\boldsymbol{H}, \quad \nabla\cdot(\mu\boldsymbol{H}) = 0, \tag{1.1a}$$

$$\nabla \times \boldsymbol{H} = -\imath\omega\varepsilon\boldsymbol{E}, \quad \nabla\cdot(\varepsilon\boldsymbol{E}) = 0, \tag{1.1b}$$

where $\imath = \sqrt{-1}$, ω is the frequency, $\boldsymbol{E}$ and $\boldsymbol{H}$ are the electric and magnetic fields, respectively. The famous Bloch theorem [28] requires that the solutions $\boldsymbol{E}$ and $\boldsymbol{H}$

*Submitted to the editors August 02, 2018.

Funding: This work was funded by MoST 105-2115-M-003-009-MY3, NSFC 11471074, MoST 106-2628-M-009-004-, MoST 107-2811-M-009-002-.

†Department of Mathematics, National Taiwan Normal University, Taipei, 116, Taiwan, (min@ntnu.edu.tw).

‡School of Mathematics, Southeast University, Nanjing 211189, People's Republic of China, (txli@seu.edu.cn).

§Department of Mathematics, National Tsing-Hua University, Hsinchu 300, Taiwan, (weideli@gapp.nthu.edu.tw).

¶Department of Applied Mathematics, National Chiao Tung University, Hsinchu 300, Taiwan, (jiawei.am05g@g2.nctu.edu.tw, wwlin@math.nctu.edu.tw, tianheng@nctu.edu.tw).

satisfy the Bloch condition (BC) [35],

$$\boldsymbol{E}(\mathbf{x}+\mathbf{a}_\ell) = \mathrm{e}^{\imath 2\pi\mathbf{k}\cdot\mathbf{a}_\ell}\boldsymbol{E}(\mathbf{x}),\ \boldsymbol{H}(\mathbf{x}+\mathbf{a}_\ell) = \mathrm{e}^{\imath 2\pi\mathbf{k}\cdot\mathbf{a}_\ell}\boldsymbol{H}(\mathbf{x}),\ \ell = 1,2,3, \tag{1.2}$$

where $\{\mathbf{a}_\ell\}_{\ell=1}^3$ are lattice translation vectors and $2\pi\mathbf{k}$ is the Bloch wave vector within the first Brillouin zone [24]. For simplicity, we only consider isotropic PC throughout this work, *i.e.*, both ε and μ are assumed to be diagonal, and further μ is set to the vacuum permeability μ_0.

Given a specific 3D PC, it can be proved that only certain nonzero real ω's can satisfy (1.1a) and (1.1b) simultaneously. Our ultimate goal is to find a few eigenvalues with smallest magnitude of the following Maxwell Eigenvalue Problem (MEP)

$$\begin{bmatrix} & \imath\nabla\times \\ -\imath\nabla\times & \end{bmatrix}\begin{bmatrix}\boldsymbol{E}\\ \boldsymbol{H}\end{bmatrix} = \omega\begin{bmatrix}\varepsilon & \\ & \mu_0\end{bmatrix}\begin{bmatrix}\boldsymbol{E}\\ \boldsymbol{H}\end{bmatrix}, \tag{1.3a}$$

$$\nabla\cdot(\varepsilon\boldsymbol{E}) = 0, \quad \nabla\cdot(\mu_0\boldsymbol{H}) = 0. \tag{1.3b}$$

To discretize the MEP (1.3), the plane-wave expansion method [20, 25, 27, 36], the multiple scattering method [18, 37], the finite-difference frequency-domain method (FDFD) [12, 13, 17, 21, 22, 39, 41, 42, 43], the finite element method [9, 10, 11, 19, 23, 30, 16, 31, 32, 33], to name a few, are available. In the case of diagonal matrix ε, the finite-difference scheme with staggered Yee grid [42], which is called Yee's scheme for short and originally proposed for time-domain simulation, is particularly attractive. In [21, 22], Yee's scheme has been used for the discretization of (1.3a), which results in a generalized eigenvalue problem (GEP). For a 3D PC, due to the divergence-free condition (1.3b), the dimension of the nullspace of the GEP accounts for one third of the total dimension. The presence of the huge nullspace will pose an extraordinary challenge to the desired solutions of the GEP. In fact, no frequency-domain method is immune to this challenge. Besides, even though only smallest few positive eigenvalues are desired, which can be calculated by the invert Lanczos method, to solve the corresponding linear system of huge size in each step of the invert Lanczos process is another challenge. In [21, 22], we have shown how we resolve these challenges in the case of the face-centered cubic (FCC) lattice and the simple cubic (SC) lattice.

In this paper, we will generalize the key results and techniques in [21, 22] to solve the MEP (1.3) for all 14 Bravais lattices. Since the triclinic lattice is the most general one, which can become other 13 Bravais lattices with corresponding constraints imposed, it suffices to consider triclinic lattice only. However, several obstacles stand out. For example, since the unit cell of the triclinic lattice is a slanted parallelepiped without any notable property, it is unclear how to formulate in matrix language the discrete single-curl operator with the BC (1.2), then it is uncertain whether the advanced nullspace free method in [21] can be applicable in this case. Although it is not uncommon to employ the oblique coordinate system in engineering and physics community, we are not convinced that all our inventions in [21, 22] can still be applicable in the oblique coordinate system, so we decide to work with the orthogonal coordinate system as before to overcome these obstacles.

We make the following contributions in this work:

- Foremost, we establish a complete and unified framework to solve the MEP (1.3) for 3D isotropic photonic crystals in all 14 Bravais lattices.
- We exhaustively classify the unit cell of the triclinic lattice which is generated by translation lattice vectors $\mathbf{a}_1, \mathbf{a}_2, \mathbf{a}_3$, and reformulate the BC within the cubic working cell accordingly (see Sec. 3 and SM2).

- We demonstrate how to cleanly discretize ∂_x, ∂_y, ∂_z including the reformulated BC into matrices C_1, C_2, C_3 with Yee's scheme (see Sec. 4). Although C_2, C_3 are usually quite complicated, they become much less daunting with our derivations. Exhaustive expressions of C_2, C_3 in the triclinic lattice and other lattices can be similarly derived (see SM2 and SM3).
- With the novel perspective that C_1, C_2, C_3 are built from shifted (block) companion matrices, the Kronecker product structure of eigenvectors of C_1, C_2, C_3 is naturally inherited from the same structure of eigenvectors of a block companion matrix. Moreover, we prove that these (block) companion matrices are unitary and in the meantime prove that $\{C_\ell^*, C_{\ell'} : \ell, \ell' = 1, 2, 3\}$ is a set of commutative matrices. By Lemma 5.4, we uncover how C_2, C_3 are constructed hierarchically from integer powers of a basic unitary companion matrix and that eigen-decompositions of $\{C_\ell^*, C_{\ell'} : \ell, \ell' = 1, 2, 3\}$ boil down to the eigen-decomposition of this unitary companion matrix (see Sec. 5).
- We show that $\mathcal{C}$ is unitarily similar to a block diagonal matrix consisting of 3-by-3 skew-symmetric blocks, and base the analytic eigen-decomposition of $\mathcal{A} = \mathcal{C}^*\mathcal{C}$ on simple factorizations of these 3-by-3 matrices, by which the orthonormal basis of the range space of $\mathcal{A}$ can be found explicitly (see Sec. 6).
- We confirm that the nullspace free method and the fast eigensolver developed previously for the FCC and SC lattices can be extended to the triclinic lattice and other Bravais lattices (see Sec. 7).

This paper is outlined as follows. In Sec. 2 an orthogonal coordinate system with which we actually work are built from non-orthogonal lattice translation vectors $\mathbf{a}_1, \mathbf{a}_2, \mathbf{a}_3$. In Sec. 3 we reformulate the BC (1.2) within the cubic working cell. In Sec. 4 we discretize $\nabla \times \boldsymbol{E}$ into matrix-vector products $\mathcal{C}E$, and discretize the MEP (1.3) into a GEP $\mathcal{A}E = \lambda\mathcal{B}E$ with $\lambda = \mu_0\omega^2$, by eliminating $\boldsymbol{H}$ in (1.3). In Sec. 5 we prove that C_1, C_2, C_3 are commutative normal matrices and obtain their analytic eigen-decomposition. In Sec. 6 we construct the factorization $(I_3 \otimes T)^*\mathcal{C}(I_3 \otimes T) = \overline{\mathcal{U}}_r\Gamma_r\mathcal{U}_r^*$ and the analytic eigen-decomposition $\mathcal{A} = \mathcal{C}^*\mathcal{C} = \mathcal{Q}_r(\Gamma_r^\top\Gamma_r)\mathcal{Q}_r^*$. In Sec. 7, the GEP is transformed into a nullspace free standard eigenvalue problem (NFSEP) $\mathcal{A}_r\widehat{E} = \lambda\widehat{E}$. For self-containedness, the fast eigensolver called FAME for the NFSEP is reviewed. In Sec. 8 the efficiency of FAME are exemplified by some numerical results. In Sec. 9 we conclude our present work.

Here we briefly introduce some notations commonly used in this work. A vector in real 3D space, which is equivalent to its coordinate representation in an orthogonal coordinate system, is marked in bold lower case. $A^\top, \overline{A}, A^*$ denote the transpose, the complex conjugate and the conjugate transpose of a matrix A, respectively. I_n denotes the identity matrix of dimension $n \in \mathbb{N}$ and e_ℓ is the ℓ-th column of I_n. $||\cdot||$ denotes the Euclidean norm. We define $\xi(\theta) := \exp(\imath 2\pi\theta)$. $\square$ABCD refers to rectangular ABCD. For convenience, we will employ MATLAB® [6] language with little explanation. For example, **floor** denotes the function of rounding to the nearest integer towards $-\infty$. Let $\mathrm{vec}(X)$ denote the vectorization operation of a matrix X of any size, *i.e.*, $X(:) = \mathrm{vec}(X)$. $A \oplus B = \mathbf{blkdiag}(A, B)$ means the direct sum of matrices A, B. $\otimes$ denotes the Kronecker product, two of whose basic properties [5] are very useful,

$$\left(Z^\top \otimes Y\right)\mathrm{vec}(X) = \mathrm{vec}(YXZ), \tag{1.4}$$

$$(X \otimes Y)(Z \otimes W) = (XZ) \otimes (YW), \tag{1.5}$$

with X, Y, Z, W being matrices of compatible sizes. Recall that A is a normal matrix, *i.e.*, $AA^* = A^*A$ if and only if A is unitarily similar to a diagonal matrix.

PROPOSITION 1.1. *[7] If A_1 and A_2 are normal with $A_1A_2 = A_2A_1$, then both A_1A_2 and $A_1 + A_2$ are also normal.*

PROPOSITION 1.2. *[3] If A is a normal matrix with one eigenpair (λ, v), then it holds that $A^*v = \overline{\lambda}v$. Furthermore, eigenspaces of a normal matrix corresponding to distinct eigenvalues are orthogonal.*

2. Lattice translation vectors, the physical cell and working cell. A crystal structure can be regarded as a lattice structure plus a basis. At present, millions of crystals are known, and each crystal has a different nature. Fortunately, there are only 7 lattice systems and 14 Bravais lattices in 3D Euclidean space [1]. The so-called primitive unit cell is a fundamental domain under the translational symmetry and contains just one lattice point [8]. The non-primitive unit cell, including body-centered, face-centered and base-centered unit cell, is preferred to reflect more complicated symmetry. Basic knowledge of the unit cell of all 7 lattice systems, 14 Bravais lattices can be found in [2].

In fact a 3D unit cell is a (slanted) parallelepiped formed by lattice translation vectors $\mathbf{a}_1, \mathbf{a}_2$ and $\mathbf{a}_3$, as illustrated in Figure 1. In the triclinic lattice there is no restriction on the length of $\mathbf{a}_1, \mathbf{a}_2, \mathbf{a}_3$ nor on the angle between any two of them, if we are able to solve the MEP (1.3) in the triclinic lattice, we can also cope with other lattices in almost the same manner. Therefore we will focus on the triclinic lattice in the main body of this work and present selective results for other lattices in SM3. For convenience, we dub the unit cell of the triclinic lattice as 3D physical cell.

In that it is inconvenient to discretize MEP (1.3) in the 3D physical cell using finite difference, we need to define a cuboid unit cell generated by new vectors $\mathbf{a}, \mathbf{b}, \mathbf{c}$ which form an orthogonal basis of $\mathbf{a}_1, \mathbf{a}_2, \mathbf{a}_3$. The general procedure to determine $\mathbf{a}, \mathbf{b}, \mathbf{c}$ is as follows:

1. Pick out the vector $\mathbf{a}_\ell$ in the set $\{\mathbf{a}_1, \mathbf{a}_2, \mathbf{a}_3\}$ that is the longest. (Here ℓ can be 1 or 2 or 3.) Let $\mathbf{a} = \mathbf{a}_\ell$ with $a = ||\mathbf{a}||$. (If more than one are equally longest, then either one can be chosen as $\mathbf{a}$.) Let $\widetilde{\mathbf{a}}_1 = \mathbf{a}$. The rest two vectors in the set $\{\mathbf{a}_1, \mathbf{a}_2, \mathbf{a}_3\}$ are renamed to $\mathbf{a}_2, \mathbf{a}_3$.
2. Set $\widehat{\mathbf{a}}_2 = \mathbf{a}_2 - \mathbf{a}(\mathbf{a}_2 \cdot \mathbf{a})/||\mathbf{a}||^2$, $\widehat{\mathbf{a}}_3 = \mathbf{a}_3 - \mathbf{a}(\mathbf{a}_3 \cdot \mathbf{a})/||\mathbf{a}||^2$. Pick out the vector $\widehat{\mathbf{a}}_\ell$ in the set $\{\widehat{\mathbf{a}}_2, \widehat{\mathbf{a}}_3\}$ that is the longer. (Here ℓ can be 2 or 3.) Let $\mathbf{b} = \widehat{\mathbf{a}}_\ell$ with $b = ||\mathbf{b}||$, and $\widetilde{\mathbf{a}}_2 = \mathbf{a}_\ell$. The other vector $\widehat{\mathbf{a}}_{\ell'}$ with $\ell' \neq \ell$ in $\{\widehat{\mathbf{a}}_2, \widehat{\mathbf{a}}_3\}$ is renamed to $\widehat{\mathbf{a}}_3$, and let $\widetilde{\mathbf{a}}_3 = \mathbf{a}_{\ell'}$.
3. Let $\mathbf{c} = \widehat{\mathbf{a}}_3 - \mathbf{b}(\widehat{\mathbf{a}}_3 \cdot \mathbf{b})/||\mathbf{b}||^2$ with $c = ||\mathbf{c}||$.

Clearly, the resulting $\mathbf{a}, \mathbf{b}, \mathbf{c}$ are mutually orthogonal, and $\mathbf{b} \times \mathbf{a} = \widetilde{\mathbf{a}}_2 \times \widetilde{\mathbf{a}}_1$, $\mathbf{c} \cdot (\mathbf{a} \times \mathbf{b}) = \widetilde{\mathbf{a}}_3 \cdot (\widetilde{\mathbf{a}}_1 \times \widetilde{\mathbf{a}}_2)$. On the other hand, by letting

$$\eta_1 = \widetilde{\mathbf{a}}_2 \cdot \mathbf{a}/a^2, \quad \eta_2 = \widetilde{\mathbf{a}}_3 \cdot \mathbf{a}/a^2, \quad \eta_3 = \widetilde{\mathbf{a}}_3 \cdot \mathbf{b}/b^2, \tag{2.1}$$

vectors $\widetilde{\mathbf{a}}_1, \widetilde{\mathbf{a}}_2, \widetilde{\mathbf{a}}_3$ can be expanded by normalized $\mathbf{a}, \mathbf{b}, \mathbf{c}$ as follows:

$$\begin{aligned}
[\widetilde{\mathbf{a}}_1, \widetilde{\mathbf{a}}_2, \widetilde{\mathbf{a}}_3] &= \left[\frac{\mathbf{a}}{a}, \frac{\mathbf{b}}{b}, \frac{\mathbf{c}}{c}\right] \begin{bmatrix} a & & \\ & b & \\ & & c \end{bmatrix} \begin{bmatrix} 1 & -\eta_1 & \eta_1\eta_3 - \eta_2 \\ 0 & 1 & -\eta_3 \\ 0 & 0 & 1 \end{bmatrix}^{-1} \\
&= \left[\frac{\mathbf{a}}{a}, \frac{\mathbf{b}}{b}, \frac{\mathbf{c}}{c}\right] \begin{bmatrix} a & a\eta_1 & a\eta_2 \\ 0 & b & b\eta_3 \\ 0 & 0 & c \end{bmatrix} = \left[\frac{\mathbf{a}}{a}, \frac{\mathbf{b}}{b}, \frac{\mathbf{c}}{c}\right] \begin{bmatrix} a_1 & a_2\cos\phi_3 & a_3\cos\phi_2 \\ 0 & a_2\sin\phi_3 & a_3\ell_2 \\ 0 & 0 & a_3\ell_3 \end{bmatrix},
\end{aligned} \tag{2.2}$$

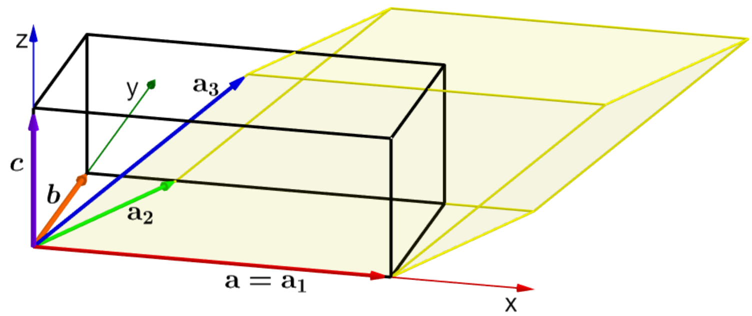

FIG. 1. *Illustration of the 3D physical cell and working cell of the triclinic lattice.*

where $a_i := ||\widetilde{\mathbf{a}}_i||$, ϕ_j is the angle between $\widetilde{\mathbf{a}}_i$ and $\widetilde{\mathbf{a}}_k$, $i, j, k = 1, 2, 3, i \neq j \neq k$,

$$\ell_2 = (\cos\phi_1 - \cos\phi_3 \cos\phi_2) / \sin\phi_3, \quad \ell_3 = \sqrt{\sin^2\phi_2 - \ell_2^2}.$$

Especially, we always have $a_3|\ell_2| \leq a_2 \sin\phi_3$.

Remark 2.1. Conventionally, in the crystallography database $\mathbf{a}_1, \mathbf{a}_2, \mathbf{a}_3$ are specified by their coordinates in the Cartesian orthogonal coordinate system which is, to avoid confusion, named as the prior orthogonal coordinate system in our work. Given such a 3-by-3 real matrix $[\mathbf{a}_1, \mathbf{a}_2, \mathbf{a}_3]$, we can call the subroutine such as the function **qr** of MATLAB® for QR factorization with column pivoting to find the orthonormal basis of $\mathbf{a}_1, \mathbf{a}_2, \mathbf{a}_3$, which yields $\pm\mathbf{a}/a, \pm\mathbf{b}/b, \pm\mathbf{c}/c$ with the same $\mathbf{a}, \mathbf{b}, \mathbf{c}$ defined above.

However, there is one important variation of the procedure above in other Bravais lattices than the triclinic lattice. That is, if, for example, $\mathbf{a}_3 \perp \mathbf{a}_1$ and $\mathbf{a}_3 \perp \mathbf{a}_2$ but $\mathbf{a}_1 \not\perp \mathbf{a}_2$, then we always choose $\mathbf{c} = \mathbf{a}_3$ and $\mathbf{a}$ as the longer one in $\{\mathbf{a}_1, \mathbf{a}_2\}$. The reason to do so will be clear later on.

Identifying normalized $\mathbf{a}, \mathbf{b}, \mathbf{c}$ as unit vectors of x-,y-,z-axes of an orthogonal coordinate system, we will work mainly in the cuboid unit cell $\mathbb{D} = \{x\mathbf{a}/a + y\mathbf{b}/b + z\mathbf{c}/c \in \mathbb{R}^3 : x \in [0, a], y \in [0, b], z \in [0, c]\}$, dubbed as the 3D working cell. To convey basic techniques of our framework of modeling of 3D PCs, we just work on one specific case where $\phi_2, \phi_3 < \pi/2$, $\ell_2 > 0$, $a_3 \cos\phi_2 \geq a_2 \cos\phi_3$, in the main body of this work.

Remark 2.2. The orthogonal coordinate system with x-,y-,z-axes can be either right-handed if $\widetilde{\mathbf{a}}_3 \cdot (\widetilde{\mathbf{a}}_1 \times \widetilde{\mathbf{a}}_2) > 0$ or left-handed if $\widetilde{\mathbf{a}}_3 \cdot (\widetilde{\mathbf{a}}_1 \times \widetilde{\mathbf{a}}_2) < 0$. Anyhow, in our work the bottom surface of $\mathbb{D}$ is always the one through the origin, while the top surface of $\mathbb{D}$ is always the one away from the origin. Our formulation in this work will be largely independent of the orientation of the axes.

3. BC within the working cell. Hereafter, for simplicity, we assume $\widetilde{\mathbf{a}}_1, \widetilde{\mathbf{a}}_2, \widetilde{\mathbf{a}}_3$ are just $\mathbf{a}_1, \mathbf{a}_2, \mathbf{a}_3$. Viewed in the 3D physical cell spanned by $\mathbf{a}_1, \mathbf{a}_2, \mathbf{a}_3$, the BC (1.2) is very clear and is naturally compatible with the periodicity of a PC along $\mathbf{a}_1, \mathbf{a}_2, \mathbf{a}_3$. However, in the 3D working cell, the formulation of the BC (1.2) needs some effort.

For convenience, given $\mathbf{v} \in \mathbb{R}^3$, the translation operator $\mathcal{T}_\mathbf{v}$ is defined as $\mathcal{T}_\mathbf{v}(\mathbf{x}) := \mathbf{x} + \mathbf{v}$, for any $\mathbf{x} \in \mathbb{R}^3$. Clearly, $\mathcal{T}_{\mathbf{v}_1+\mathbf{v}_2} = \mathcal{T}_{\mathbf{v}_1}\mathcal{T}_{\mathbf{v}_2} = \mathcal{T}_{\mathbf{v}_2}\mathcal{T}_{\mathbf{v}_1}$.

Since $\mathbf{a}_1 = \mathbf{a}$, the BC (1.2) along the x-axis is trivial, *i.e.*,

$$\boldsymbol{E}(\mathbf{x}) = \xi(\mathbf{k} \cdot (\mathbf{x} - \mathcal{T}_{-\mathbf{a}}(\mathbf{x})))\boldsymbol{E}(\mathcal{T}_{-\mathbf{a}}(\mathbf{x})), \quad \mathbf{x} = (x, y, z) \in \mathbb{D}. \tag{3.1}$$

Note that $\xi(\theta) = \exp(\imath 2\pi\theta)$. However, the BC (1.2) along the y- and z-axes are nontrivial. For derivations in this work, we only need to consider the relation between $\boldsymbol{E}((x,y,c))$ and $\boldsymbol{E}(\mathcal{T}_{-\mathbf{c}}((x,y,c)))$ with $(x,y,c) \in \mathbb{D}$, and that between $\boldsymbol{E}((x,b,z))$ and $\boldsymbol{E}(\mathcal{T}_{-\mathbf{b}}((x,b,z)))$ with $(x,b,z) \in \mathbb{D}$. Given $\mathbf{x} = (x,y,0) \in \mathbb{D}$, we just think of $(x_2,y_2,0)$ as the image of $\mathbf{x}+\mathbf{c}$ (a point of the top surface of $\mathbb{D}$) under $\mathcal{T}_{-\mathbf{a}_3}$, as shown in Figure 2(a), and $\mathbf{a}_3^{\perp} = \mathbf{a}_3 - \mathbf{c}$ is the projection of $\mathbf{a}_3$ onto the xy-plane, then the BC (1.2) along the z-axis could be

$$\begin{aligned} \boldsymbol{E}(\mathcal{T}_{-\mathbf{c}}((x,y,c))) &= \xi\left(\mathbf{k}\cdot((x,y,0)) - (x_2,y_2,0)\right)\boldsymbol{E}((x_2,y_2,0)) \\ &= \xi\left(\mathbf{k}\cdot((x,y,0)) - \mathcal{T}_{-\mathbf{a}_3}((x,y,c))\right)\boldsymbol{E}(\mathcal{T}_{-\mathbf{a}_3}((x,y,c))), \end{aligned} \tag{3.2}$$

with $(x,y,0) - \mathcal{T}_{-\mathbf{a}_3}((x,y,c))$ being integer multiples of $\mathbf{a}_1, \mathbf{a}_2$.

In Figure 2(b), $\square \mathrm{OR}_1\mathrm{R}_2\mathrm{R}_3$ is the bottom surface of $\mathbb{D}$, while $\square \mathrm{R}_4\mathrm{R}_5\mathrm{R}_6\mathrm{R}_7$ is the image of the top surface of $\mathbb{D}$ under $\mathcal{T}_{-\mathbf{a}_3}$ and overlaps with patch I of the former. In short, there should be four patches within $\square \mathrm{OR}_1\mathrm{R}_2\mathrm{R}_3$, namely, $\mathrm{I}, \mathrm{II}, \mathrm{III}, \mathrm{IV}$, and these four patches, equipped with different linear mappings $\mathcal{T}_0, \mathcal{T}_{-\mathbf{a}_1}, \mathcal{T}_{-\mathbf{a}_1-\mathbf{a}_2}, \mathcal{T}_{-\mathbf{a}_2}$ are mapped to four patches $\widetilde{\mathrm{I}}$, $\widetilde{\mathrm{II}}$, $\widetilde{\mathrm{III}}$, $\widetilde{\mathrm{IV}}$, respectively, within $\square \mathrm{R}_4\mathrm{R}_5\mathrm{R}_6\mathrm{R}_7$. We refer the reader to SM1 to see how to obtain the patches and the mapping in Figure 2(b). Then we can establish the correct BC (1.2) within the bottom surface of $\mathbb{D}$, which specifies x_2, y_2 in (3.2). Letting $\mathbf{x} = (x,y,0) \in \mathbb{D}$, given the conditions specified in Sec. 2, it holds that

$$\boldsymbol{E}(\mathbf{x}) = \begin{cases} \boldsymbol{E}(\mathbf{x}), & \text{if } \mathbf{x} \in \mathrm{I} \\ \xi(\mathbf{k}\cdot\mathbf{a}_1)\boldsymbol{E}(\mathbf{x}-\mathbf{a}_1), & \text{if } \mathbf{x} \in \mathrm{II} \\ \xi(\mathbf{k}\cdot(\mathbf{a}_1+\mathbf{a}_2))\boldsymbol{E}((\mathbf{x}-\mathbf{a}_1-\mathbf{a}_2)), & \text{if } \mathbf{x} \in \mathrm{III} \\ \xi(\mathbf{k}\cdot\mathbf{a}_2)\boldsymbol{E}(\mathbf{x}-\mathbf{a}_2), & \text{if } \mathbf{x} \in \mathrm{IV}. \end{cases} \tag{3.3}$$

In passing, considering that $\boldsymbol{E}(\mathcal{T}_{\mathbf{a}_3}(\mathbf{x})) = \xi(\mathbf{k}\cdot\mathbf{a}_3)\boldsymbol{E}(\mathbf{x})$, we can of course add $\mathbf{a}_3$ to the argument of $\boldsymbol{E}$ on the right hand side of (3.3) with updated prefactor. Depending on combinations of various $a_2,\ a_3,\ \phi_3,\ \phi_2,\ \ell_2$, (3.3) could be quite different. In SM2, we reformulate the BC (1.2) for altogether 16 cases, including (3.3).

As for the BC (1.2) along the y-axis, we observe that $\boldsymbol{E}(\mathcal{T}_{-\mathbf{b}}((x,b,z)))$ with $(x,b,z) \in \mathbb{D}$ does not involve the influence of $\mathcal{T}_{\mathbf{a}_3}$, we can just let $z = 0$ here for simplicity. Letting $\mathbf{x} = (x,b,0) \in \mathbb{D}$, we have the BC (1.2) along the y-axis for different segments of $\mathrm{R}_3\mathrm{R}_2$ shown in Figure 2(b):

$$\boldsymbol{E}(\mathbf{x}) = \begin{cases} \xi(\mathbf{k}\cdot\mathbf{a}_2)\boldsymbol{E}(\mathcal{T}_{-\mathbf{a}_2}(\mathbf{x})), & \text{if } \mathbf{x} \in \mathrm{R}_8\mathrm{R}_2 \\ \xi(\mathbf{k}\cdot(\mathbf{a}_2-\mathbf{a}_1))\boldsymbol{E}(\mathcal{T}_{\mathbf{a}_1-\mathbf{a}_2}(\mathbf{x})), & \text{if } \mathbf{x} \in \mathrm{R}_3\mathrm{R}_8. \end{cases} \tag{3.4}$$

4. Matrix Representation of the Discretized Single-Curl.

Let's first discretize $\nabla \times \boldsymbol{E}$ in (1.3a) with finite-difference scheme, without worrying about (1.3b) at the moment. Below we will use quantities in (2.2).

Given $n_1, n_2, n_3 \in \mathbb{N}$, we can have a uniform grid along the x-,y-,z-axes of our 3D working cell $\mathbb{D}$, respectively, with constant grid spacing

$$\delta_x = a/n_1, \quad \delta_y = b/n_2, \quad \delta_z = c/n_3,$$

respectively. Each component of the vector $\boldsymbol{E}(\mathbf{x}) = [E_1(\mathbf{x}), E_2(\mathbf{x}), E_3(\mathbf{x})]^\top$ could be sampled at different points in general. Hence we assume that $E_\ell(\mathbf{x})$ is sampled at

$$\mathbf{x}_\ell(i,j,k) = \mathbf{x}_\ell(0,0,0) + (i\delta_x, j\delta_y, k\delta_z), \tag{4.1}$$

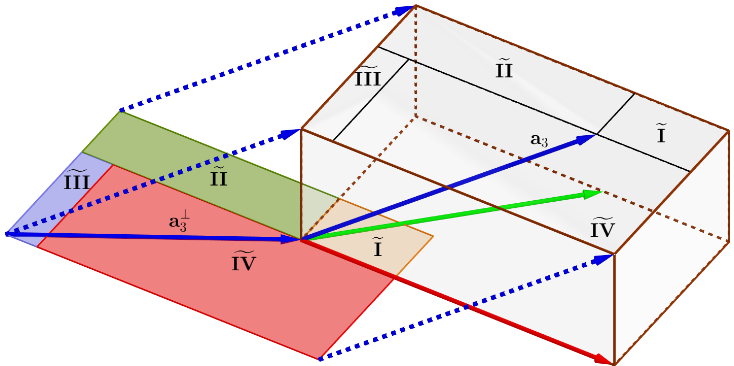

(a) The action of $\mathcal{T}_{-\mathbf{a}_3}$ on the top surface of $\mathbb{D}$.

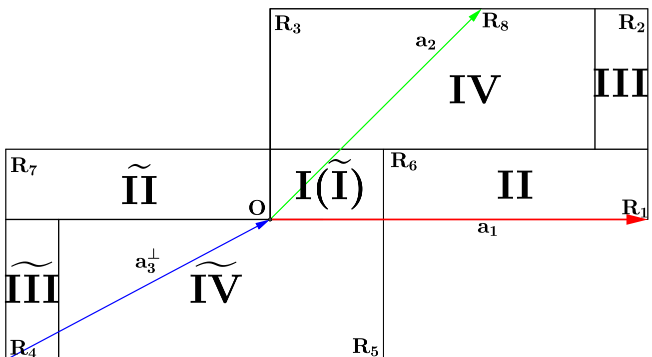

(b) Correspondence between different patches of the bottom surface of $\mathbb{D}$ and those of $\mathcal{T}_{-\mathbf{a}_3}((x,y,c))$.

FIG. 2. *Illustration of* (3.3) *between the bottom surface of* $\mathbb{D}$ *and* $\mathcal{T}_{-\mathbf{a}_3}((x,y,c))$.

where $\mathbf{x}_\ell(0,0,0)$ will be specified later in this section and $\ell = 1,2,3,\ i = 0,1,\ldots,n_1-1,\ j = 0,1,\ldots,n_2-1,\ k = 0,1,\ldots,n_3-1$. Unless otherwise stated, in this section i,j,k always take on these values.

Given ℓ, the three-way array $E_\ell(\mathbf{x}_\ell(:,:,:))$ of number of elements $n = n_1n_2n_3$ is arranged in the column-major order, *i.e.*, the first index varies fastest while the last varies slowest. For convenience, $E_\ell(\mathbf{x}_\ell(:,:,:))$, $\ell = 1,2,3$, are stored in a column vector $E = [E_1(:); E_2(:); E_3(:)]$.

Part I. Discrete $\partial_x E_\ell$. Since the BC (3.1) is very similar to 1D case, using matrix language, we recast

$$\frac{E_\ell(\mathbf{x}_\ell(i+1,j,k)) - E_\ell(\mathbf{x}_\ell(i,j,k))}{\delta_x}, \quad \ell = 2,3, \tag{4.2}$$

into $C_1E_\ell(:)$, where

$$C_1 = I_{n_3} \otimes I_{n_2} \otimes \frac{K_1 - I_{n_1}}{\delta_x}, \quad K_1 = \begin{bmatrix} 0 & I_{n_1-1} \\ \xi(\mathbf{k}\cdot\mathbf{a}_1) & 0 \end{bmatrix}. \tag{4.3}$$

Part II. Discrete $\partial_y E_\ell$. The BC (3.4) holds for continuous $\mathbf{x}$, however, if we want to recast

$$\frac{E_\ell(\mathbf{x}_\ell(i,j+1,k)) - E_\ell(\mathbf{x}_\ell(i,j,k))}{\delta_y}, \quad \ell = 1,3, \tag{4.4}$$

into a matrix-vector product, we need the discretized version of (3.4).

Although in Figure 3, with modulo operation defined in SM1, we have in principle $\mathrm{R}_8 \equiv \mathrm{O} \mod \mathbf{a}_2$, it is very rare that R_8 coincides exactly with any of the grid point in a given uniform grid within $\mathrm{R}_3\mathrm{R}_2$. As an expediency to resolve this mismatching, we stipulate that the rightmost grid point within $\mathrm{R}_3\mathrm{R}_8$ be the substitute of R_8. Putting it differently, when $\phi_3 < \pi/2$, since the number of grid points in $\mathrm{R}_3\mathrm{R}_8$ is $m_1 = \mathbf{floor}\left((a_2 \cos\phi_3)/\delta_x\right)$, then $\mathbf{x}_\ell(m_1, n_2, k) \equiv \mathbf{x}_\ell(0, 0, k) \mod \mathbf{a}_2$ holds by force, ignoring the discretization error.

In accordance with two cases in (3.4), $E_\ell(\mathbf{x}_\ell(:, n_2, k))$, a column vector of length n_1, is partitioned into 2 blocks, and the discretized BC (3.4) is

$$E_\ell(\mathbf{x}_\ell(:, n_2, k)) = \xi(\mathbf{k}\cdot\mathbf{a}_2) J_2 E_\ell(\mathbf{x}_\ell(:, 0, k)), \tag{4.5}$$

$$J_2 = \begin{bmatrix} 0 & \xi(-\mathbf{k}\cdot\mathbf{a}_1) I_{m_1} \\ I_{n_1-m_1} & 0 \end{bmatrix} \in \mathbb{C}^{n_1\times n_1}. \tag{4.6}$$

Finally, (4.4) is recast into $C_2 E_\ell(:)$, where

$$C_2 = I_{n_3} \otimes \frac{K_2 - I_{n_1 n_2}}{\delta_y}, \quad K_2 = \begin{bmatrix} 0 & I_{n_2-1}\otimes I_{n_1} \\ \xi(\mathbf{k}\cdot\mathbf{a}_2) J_2 & 0 \end{bmatrix}. \tag{4.7}$$

In passing, when $\phi_3 > \pi/2$, m_1 and J_2 are specified in SM2.

Part III. Discrete $\partial_z E_\ell$. If we want to recast

$$\frac{E_\ell(\mathbf{x}_\ell(i, j, k+1)) - E_\ell(\mathbf{x}_\ell(i, j, k))}{\delta_z}, \quad \ell = 1, 2, \tag{4.8}$$

into a matrix-vector product, we need to know how $E_\ell(\mathbf{x}_\ell(:, :, n_3))$ is related to $E_\ell(\mathbf{x}_\ell(:, :, 0))$ from the BC (3.3).

We have following observations about Figure 3,

- $\overline{\mathrm{R}_9\mathrm{R}_6} = a_1 - a_3\cos\phi_2$, $\overline{\mathrm{R}_9\widehat{\mathrm{R}}_5} = a - (a_3\cos\phi_2 - a_2\cos\phi_3)$,
- $\overline{\mathrm{R}_3\mathrm{R}_9} = a_3\ell_2$, $\overline{\mathrm{R}_9\mathrm{O}} = a_2\sin\phi_3 - a_3\ell_2$.

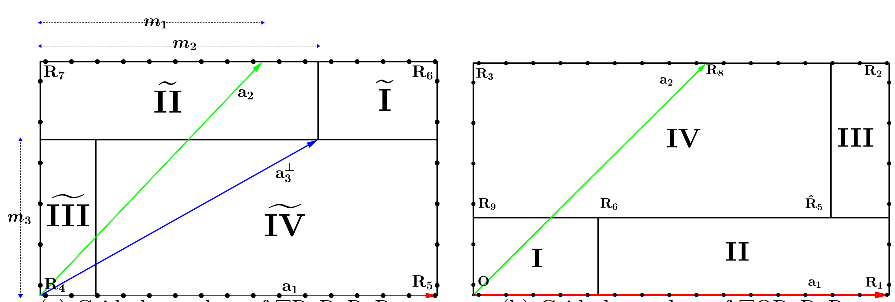

(a) Grid along edges of $\square\mathrm{R}_4\mathrm{R}_5\mathrm{R}_6\mathrm{R}_7$. (b) Grid along edges of $\square\mathrm{O}\mathrm{R}_1\mathrm{R}_2\mathrm{R}_3$.

FIG. 3. *Illustration of uniform grid in the top and bottom surface of* $\mathbb{D}$.

Again, it is very rare that vertices of any patch in Figure 3 coincide exactly with any of the grid point for a given uniform mesh in $\square\mathrm{O}\mathrm{R}_1\mathrm{R}_2\mathrm{R}_3$. Define

$$m_2 = \mathbf{floor}((a_3\cos\phi_2)/\delta_x), \quad m_3 = \mathbf{floor}(a_3\ell_2/\delta_y), \quad m_4 = m_2 - m_1, \tag{4.9}$$

then along the x-axis $\mathrm{R}_9\mathrm{R}_6$ contains $n_1 - m_2$ grid points and $\mathrm{R}_9\widehat{\mathrm{R}}_5$ contains $n_1 - m_4$ grid points, while along the y-axis $\mathrm{R}_3\mathrm{R}_9$ contains m_3 grid points and $\mathrm{R}_9\mathrm{O}$ contains $n_2 - m_3$ grid points.

In accordance with Figure 3, matrices $E_\ell(\mathbf{x}_\ell(:,:,0))$ and $E_\ell(\mathcal{T}_{-\mathbf{a}_3}(\mathbf{x}_\ell(:,:,n_3)))$ of size $n_1 \times n_2$ are partitioned into four blocks,

$$E_\ell(\mathbf{x}_\ell(:,:,0)) = \begin{bmatrix} E_{\mathrm{I}} & E_{\mathrm{IV}} \\ E_{\mathrm{II}} & E_{\mathrm{III}} \end{bmatrix}, \quad E_\ell(\mathcal{T}_{-\mathbf{a}_3}(\mathbf{x}_\ell(:,:,n_3))) = \begin{bmatrix} E_{\widetilde{\mathrm{III}}} & E_{\widetilde{\mathrm{II}}} \\ E_{\widetilde{\mathrm{IV}}} & E_{\widetilde{\mathrm{I}}} \end{bmatrix}.$$

The size of each block becomes transparent in (4.10), (4.11), (4.12) below. Then the discretized version of (3.3) is as follows:

$$\begin{bmatrix} E_{\widetilde{\mathrm{II}}} \\ E_{\widetilde{\mathrm{I}}} \end{bmatrix} = \begin{bmatrix} 0 & \xi(-\mathbf{k}\cdot\mathbf{a}_1) I_{m_2} \\ I_{n_1-m_2} & 0 \end{bmatrix} \begin{bmatrix} E_{\mathrm{I}} \\ E_{\mathrm{II}} \end{bmatrix} I_{n_2-m_3}, \tag{4.10}$$

$$\begin{bmatrix} E_{\widetilde{\mathrm{III}}} \\ E_{\widetilde{\mathrm{IV}}} \end{bmatrix} = \begin{bmatrix} 0 & \xi(-\mathbf{k}\cdot\mathbf{a}_1) I_{m_4} \\ I_{n_1-m_4} & 0 \end{bmatrix} \begin{bmatrix} E_{\mathrm{IV}} \\ E_{\mathrm{III}} \end{bmatrix} \xi(-\mathbf{k}\cdot\mathbf{a}_2) I_{m_3}, \tag{4.11}$$

$$\begin{bmatrix} E_{\mathrm{IV}} & E_{\mathrm{I}} \\ E_{\mathrm{III}} & E_{\mathrm{II}} \end{bmatrix} = I_{n_1} \begin{bmatrix} E_{\mathrm{I}} & E_{\mathrm{IV}} \\ E_{\mathrm{II}} & E_{\mathrm{III}} \end{bmatrix} \begin{bmatrix} 0 & I_{n_2-m_3} \\ I_{m_3} & 0 \end{bmatrix}. \tag{4.12}$$

Actually $\mathrm{vec}(E_\ell(\mathbf{x}_\ell(:,:,0)))$ can be seen as the vertical concatenation of $\mathrm{vec}\left([E_{\mathrm{I}}; E_{\mathrm{II}}]\right)$ and $\mathrm{vec}\left([E_{\mathrm{IV}}; E_{\mathrm{III}}]\right)$, so can $\mathrm{vec}(E_\ell(\mathcal{T}_{-\mathbf{a}_3}(\mathbf{x}_\ell(:,:,n_3))))$.

Finally, with (4.10), (4.11), (4.12), (1.4), we can recast (4.8) into $C_3 E_\ell(:)$, where

$$C_3 = \frac{K_3 - I_n}{\delta_z}, \quad K_3 = \begin{bmatrix} 0 & I_{n_3-1} \otimes I_{n_2} \otimes I_{n_1} \\ \xi(\mathbf{k}\cdot\mathbf{a}_3) J_3 & 0 \end{bmatrix} \in \mathbb{C}^{n\times n}, \tag{4.13}$$

$$\begin{aligned} J_3 &= \begin{bmatrix} \xi(-\mathbf{k}\cdot\mathbf{a}_2) I_{m_3} \otimes \begin{bmatrix} 0 & \xi(-\mathbf{k}\cdot\mathbf{a}_1) I_{m_4} \\ I_{n_1-m_4} & 0 \end{bmatrix} & \\ & I_{n_2-m_3} \otimes \begin{bmatrix} 0 & \xi(-\mathbf{k}\cdot\mathbf{a}_1) I_{m_2} \\ I_{n_1-m_2} & 0 \end{bmatrix} \end{bmatrix} \times \\ &\quad \left(\begin{bmatrix} 0 & I_{n_2-m_3} \\ I_{m_3} & 0 \end{bmatrix}^\top \otimes I_{n_1} \right) \\ &= \begin{bmatrix} & \xi(-\mathbf{k}\cdot\mathbf{a}_2) I_{m_3} \otimes \begin{bmatrix} 0 & \xi(-\mathbf{k}\cdot\mathbf{a}_1) I_{m_4} \\ I_{n_1-m_4} & 0 \end{bmatrix} \\ I_{n_2-m_3} \otimes \begin{bmatrix} 0 & \xi(-\mathbf{k}\cdot\mathbf{a}_1) I_{m_2} \\ I_{n_1-m_2} & 0 \end{bmatrix} & \end{bmatrix}. \end{aligned} \tag{4.14}$$

Different expression of J_3 can be found in SM2 for different reformulated BC (1.2). Particularly, if $\mathbf{c} = \mathbf{a}_3$, J_3 is simplified to $I_{n_1 n_2}$.

Part IV. Discrete $\partial_x H_\ell, \partial_y H_\ell, \partial_z H_\ell$. In order to preserve the Hermiticity of the operator on the left hand side of the MEP (1.3) at the discrete level, the single-curl operator in (1.1b) should be discretized slightly differently. We will not detail the derivations, but just present the results. Specifically, the discretized version of (3.1), (3.3) and (3.4) can be immediately written down verbatim in terms of $\boldsymbol{H}(\mathbf{x})$ in place of $\boldsymbol{E}(\mathbf{x})$, and we assume that $H_\ell(\mathbf{x})$ is sampled at

$$\mathbf{y}_\ell(i,j,k) = \mathbf{y}_\ell(0,0,0) + (i\delta_x, j\delta_y, k\delta_z), \quad \ell = 1,2,3, \tag{4.15}$$

where $\mathbf{y}_\ell(0,0,0)$ will be specified later in this section. Then we can recast

$$\frac{H_\ell(\mathbf{y}_\ell(i,j,k)) - H_\ell(\mathbf{y}_\ell(i-1,j,k))}{\delta_x}, \quad \ell = 2,3, \tag{4.16}$$

$$\frac{H_\ell(\mathbf{y}_\ell(i,j,k)) - H_\ell(\mathbf{y}_\ell(i,j-1,k))}{\delta_y}, \quad \ell = 1,3, \tag{4.17}$$

$$\frac{H_\ell(\mathbf{y}_\ell(i,j,k)) - H_\ell(\mathbf{y}_\ell(i,j,k-1))}{\delta_z}, \quad \ell = 1,2, \tag{4.18}$$

into $-C_1^* H_\ell(:)$, $-C_2^* H_\ell(:)$ and $-C_3^* H_\ell(:)$, respectively.

Part V. Yee's scheme and discretized MEP (1.3). To return to the famous Yee's scheme, $\mathbf{x}_\ell(0,0,0)$, $\mathbf{y}_\ell(0,0,0)$ in (4.1), (4.15), respectively, are set to

$$\mathbf{x}_1(0,0,0) = (\delta_x/2, 0, 0),\ \mathbf{x}_2(0,0,0) = (0, \delta_y/2, 0),\ \mathbf{x}_3(0,0,0) = (0,0,\delta_z/2),$$
$$\mathbf{y}_1(0,0,0) = (0,\delta_y,\delta_z)/2,\ \mathbf{y}_2(0,0,0) = (\delta_x, 0, \delta_z)/2,\ \mathbf{y}_3(0,0,0) = (\delta_x,\delta_y,0)/2.$$

In addition, since $\varepsilon(\mathbf{x})$ is assumed to be diagonal, then with $\mathbf{x}_\ell$ defined in (4.1) we can define the following positive diagonal matrix $\mathcal{B}$,

$$\mathcal{B} = \mathbf{diag}([\mathrm{vec}(\varepsilon(\mathbf{x}_1(:,:,:))); \mathrm{vec}(\varepsilon(\mathbf{x}_2(:,:,:))); \mathrm{vec}(\varepsilon(\mathbf{x}_3(:,:,:)))]).$$

With Yee's staggered grid $\mathbf{x}_\ell(:,:,:)$, $\mathbf{y}_\ell(:,:,:)$ specified above, using (4.2), (4.4), (4.8) and (4.16), (4.17), (4.18), it can be proved that the divergence free condition (1.3b) is automatically satisfied, hence, (1.3b) will not show up explicitly in the following discretized MEP (1.3):

$$\mathcal{A}E = \lambda \mathcal{B} E, \quad \lambda = \mu_0 \omega^2, \quad \mathcal{A} = \mathcal{C}^* \mathcal{C}, \tag{4.19}$$

$$\mathcal{C} = \begin{bmatrix} 0 & -C_3 & C_2 \\ C_3 & 0 & -C_1 \\ -C_2 & C_1 & 0 \end{bmatrix}. \tag{4.20}$$

This is the superiority of Yee's scheme.

5. Eigen-decomposition of partial derivative operators. In order to determine the nullspace and range space of $\mathcal{A}$ in (4.19) analytically, following [21], we need eigen-decompositions of K_1, K_2, K_3. The derivations which closely follow [21, 22] can certainly be developed in our case, albeit much lengthy and boring. Another reason that makes us turn away from derivations in [21, 22] is that they can not explain why the Kronecker product structure shows up in K_2's and K_3's eigenvectors.

It has been proved in the case of the FCC lattice [21] that C_1, C_2, C_3 defined in Sec. 3 commute with each other and are simultaneously diagonalized by the same unitary matrix. This reminds us that C_1, C_2, C_3 in our case are probably commutative normal matrices, too. Below we will prove this guess, but not by tedious verification of $C_\ell^* C_\ell = C_\ell C_\ell^*$, $\ell = 1,2,3$.

In this section, we will partially uncover the underlying cause of the two facts that eigenvectors of K_2, K_3 admit of Kronecker product and that C_1, C_2, C_3 are commutative normal matrices, which are both related to (block) companion matrices.

LEMMA 5.1. *Given $q \in \mathbb{N}$, let $p(t) = \sum_{j=0}^{q-1} p_j t^j + t^q$ be a q-th degree complex monic polynomial, then $p(\lambda) = \det(\lambda I_q - C_F(p))$ with*

$$C_F(p) = \begin{bmatrix} 0 & 1 & \cdots & 0 \\ \vdots & \vdots & \ddots & \vdots \\ 0 & 0 & \cdots & 1 \\ -p_0 & -p_1 & \cdots & -p_{q-1} \end{bmatrix}$$

and the eigenvector of $C_F(p)$ *corresponding to the eigenvalue* λ_j *is* $[1, \lambda_j, \cdots, \lambda_j^{q-1}]^\top$, $j = 1, 2, \cdots, q$. *Moreover, if* $p_1 = \cdots = p_{q-1} = 0$, $|p_0| = 1$, *then* $C_F(p)^* C_F(p) = I_q$.

Since Lemma 5.1 can be directly verified, we skip its proof. Letting $p(t) = t^{n_1} - \xi(\mathbf{k} \cdot \mathbf{a}_1)$ in Lemma 5.1, we have the following theorem.

THEOREM 5.2 ([21]). K_1 *in* (4.3) *is unitary and satisfies* $K_1 X_i = \xi(\theta_\mathbf{a})\xi(i/n_1)X_i$ *where* $\theta_\mathbf{a} = \mathbf{k} \cdot \mathbf{a}/n_1 = \mathbf{k} \cdot \mathbf{a}_1/n_1$, $i = 1, \ldots, n_1$,

$$X_i = \left[1, \xi(\theta_\mathbf{a})\xi\left(\frac{i}{n_1}\right), \cdots, \xi((n_1-1)\theta_\mathbf{a})\xi\left(\frac{(n_1-1)i}{n_1}\right)\right]^\top. \tag{5.1}$$

LEMMA 5.3 ([15]). *Given* $q, m \in \mathbb{N}$, *let* $M(\lambda) = \sum_{j=0}^{q-1} \lambda^j M_j + \lambda^q I_m$ *with* $M_j \in \mathbb{C}^{m\times m}$, $j = 0, 1, \cdots, q-1$, *then* $\det M(\lambda) = \det(\lambda I_{mq} - C_{BF}(M))$ *with*

$$C_{BF}(M) = \begin{bmatrix} 0 & I_m & \cdots & 0 \\ \vdots & \vdots & \ddots & \vdots \\ 0 & 0 & \cdots & I_m \\ -M_0 & -M_1 & \cdots & -M_{q-1} \end{bmatrix}.$$

Particularly, if $v \in \mathbb{C}^m$ *and* $\lambda_0 \in \mathbb{C}$ *satisfy* $M(\lambda_0)v = 0$, *then the eigenvector of* $C_{BF}(M)$ *corresponding to eigenvalue* λ_0 *is* $[1, \lambda_0, \lambda_0^2, \cdots, \lambda_0^{q-1}]^\top \otimes v$. *Moreover, if* $M_1 = \cdots = M_{q-1} = 0$, $M_0^* M_0 = I_m$, *then* $C_{BF}(M)^* C_{BF}(M) = I_{mq}$.

Now in Lemma 5.3 letting $M(\lambda) = \lambda^{n_2} I_{n_1} - \xi(\mathbf{k} \cdot \mathbf{a}_2)J_2$, we see that $C_{BF}(M)$ is just K_2 in (4.7) and eigenpairs of K_2 are made from those of J_2 in (4.6). Specifically, if (ν_0, v) is an eigenpair of J_2, then $\nu = (\xi(\mathbf{k} \cdot \mathbf{a}_2)\nu_0)^{1/n_2}$ is an eigenvalue of K_2 with the corresponding eigenvector $[1, \nu, \nu^2, \cdots, \nu^{n_2-1}]^\top \otimes v$, where one of n_2 branches of z^{1/n_2} has been chosen. Similarly, in Lemma 5.3 letting $M(\lambda) = \lambda^{n_3} I_{n_1 n_2} - \xi(\mathbf{k} \cdot \mathbf{a}_3)J_3$, we see that eigenpairs of K_3 in (4.13) are made from those of J_3 in (4.14). Therefore, the emergence of the Kronecker product structure in eigenvectors of K_2, K_3 becomes self-evident and below we just concern about eigen-decompositions of J_2 and J_3.

Lemma 5.4 below is the crucial apparatus in this section.

LEMMA 5.4. *Given* $0 \neq \theta \in \mathbb{R}$ *and* $q_1, q_2 \in \mathbb{N}$ *and* $G \in \mathbb{C}^{q_1 \times q_1}$, *for any* $q \in Ind = \{1, 2, \ldots, q_2\}$, *we have*

$$W_{q_1 q_2}(G, \theta, q) := \begin{bmatrix} 0 & I_{q_2 - q} \otimes I_{q_1} \\ \xi(\theta) I_q \otimes G & 0 \end{bmatrix} = (W_{q_1 q_2}(G, \theta, 1))^q. \tag{5.2}$$

Proof. When $q = 1$, (5.2) is obviously true. Suppose (5.2) is true when $1 \leq q = r < q_2$, *i.e.*, $W_{q_1 q_2}(G, \theta, r) = (W_{q_1 q_2}(G, \theta, 1))^r$, then by direct multiplication,

$$W_{q_1 q_2}(G, \theta, r) W_{q_1 q_2}(G, \theta, 1) = \begin{bmatrix} 0 & I_{q_2 - r - 1} \otimes I_{q_1} \\ \xi(\theta) I_{r+1} \otimes G & 0 \end{bmatrix}$$
$$= W_{q_1 q_2}(G, \theta, r+1) = (W_{q_1 q_2}(G, \theta, 1))^{r+1}.$$

By induction, (5.2) holds for all $q \in$ Ind. ∎

COROLLARY 5.5. *With* K_1, J_2, $\theta_\mathbf{a}$, X_i *defined in* (4.3), (4.6) *and Theorem* 5.2, *respectively, we have*

$$J_2 = K_1^{-m_1}, \quad J_2^* J_2 = I_{n_1},$$

and the eigenpairs of J_2 *are* $(\xi(-m_1\theta_\mathbf{a})\xi(-im_1/n_1), X_i)$, *for* $i = 1, \ldots, n_1$.

Proof. Let $q_1 = 1$, $G = 1$, $q_2 = n_1$, $q = m_1$, $\theta = \mathbf{k}\cdot\mathbf{a}_1$ in Lemma 5.4, then $W_{q_1q_2}(G,\theta,1) = K_1$, $W_{q_1q_2}(G,\theta,m_1) = J_2^* = K_1^{m_1}$. Hence by Theorem 5.2, $J_2 = (K_1^{m_1})^* = K_1^{-m_1}$, $J_2^*J_2 = I_{n_1}$, and $J_2X_i = (\xi(-\theta_{\mathbf{a}})\xi(-i/n_1))^{m_1}X_i$. ∎

Then, as mentioned above, by Lemma 5.3, we have the following theorem.

THEOREM 5.6. *K_2 in (4.7) is unitary. With X_i defined in (5.1), K_2 satisfies*

$$K_2(Y_{ij}\otimes X_i) = \xi(\theta_{\mathbf{b},i})\xi(j/n_2)(Y_{ij}\otimes X_i),\ i = 1,\cdots,n_1,\ j = 1,\cdots,n_2,$$

where

$$\theta_{\mathbf{b},i} = \frac{1}{n_2}\left(\mathbf{k}\cdot\mathbf{b} - \frac{im_1}{n_1}\right) = \frac{1}{n_2}\left[\mathbf{k}\cdot\left(\mathbf{a}_2 - \frac{m_1}{n_1}\mathbf{a}_1\right) - \frac{im_1}{n_1}\right], \tag{5.3a}$$

$$Y_{ij} = \left[1, \xi(\theta_{\mathbf{b},i})\xi\left(\frac{j}{n_2}\right), \cdots, \xi((n_2-1)\theta_{\mathbf{b},i})\xi\left(\frac{(n_2-1)j}{n_2}\right)\right]^\top. \tag{5.3b}$$

Remark 5.7. We have the approximation $\eta_1 = m_1/n_1$ in (2.1), then $\mathbf{b} = \mathbf{a}_2 - \mathbf{a}_1 m_1/n_1$ in (5.3a) holds ignoring the discretization error.

LEMMA 5.8. *With K_1, K_2, J_3 in (4.3), (4.7), (4.14), respectively, and m_2, m_3 in (4.9), it holds that*

$$J_3 = K_2^{-m_3}\left(I_{n_2}\otimes K_1\right)^{-m_2} = \left(I_{n_2}\otimes K_1\right)^{-m_2}K_2^{-m_3}, \quad J_3^*J_3 = I_{n_1n_2}.$$

Proof. Let $q_1 = n_1$, $q_2 = n_2$, $q = m_3$, $\theta = \mathbf{k}\cdot\mathbf{a}_2$, $G = J_2$ in Lemma 5.4, with J_2 in (4.6), then $W_{q_1q_2}(G,\theta,1) = K_2$ and $W_{q_1q_2}(G,\theta,q) = K_2^{m_3}$. By Corollary 5.5,

$$\begin{aligned}
J_3^* &= \begin{bmatrix} 0 & I_{n_2-m_3}\otimes K_1^{m_2} \\ \xi(\mathbf{k}\cdot\mathbf{a}_2)I_{m_3}\otimes K_1^{m_2-m_1} & 0 \end{bmatrix} \\
&= \begin{bmatrix} 0 & I_{n_2-m_3}\otimes I_{n_1} \\ \xi(\mathbf{k}\cdot\mathbf{a}_2)I_{m_3}\otimes J_2 & 0 \end{bmatrix}\left(I_{n_2}\otimes K_1^{m_2}\right) = K_2^{m_3}\left(I_{n_2}\otimes K_1\right)^{m_2} \\
&= \left(I_{n_2}\otimes K_1^{m_2}\right)\begin{bmatrix} 0 & I_{n_2-m_3}\otimes I_{n_1} \\ \xi(\mathbf{k}\cdot\mathbf{a}_2)I_{m_3}\otimes J_2 & 0 \end{bmatrix} = \left(I_{n_2}\otimes K_1\right)^{m_2}K_2^{m_3}.
\end{aligned}$$

Hence,

$$\begin{aligned}
J_3 &= \{K_2^{m_3}\left(I_{n_2}\otimes K_1\right)^{m_2}\}^* = \left(I_{n_2}\otimes K_1\right)^{-m_2}K_2^{-m_3}, \quad J_3^*J_3 = I_{n_1n_2}, \\
J_3 &= \{\left(I_{n_2}\otimes K_1\right)^{m_2}K_2^{m_3}\}^* = K_2^{-m_3}\left(I_{n_2}\otimes K_1\right)^{-m_2}.
\end{aligned}$$
∎

COROLLARY 5.9. *It holds that $K_2\left(I_{n_2}\otimes K_1\right) = \left(I_{n_2}\otimes K_1\right)K_2$. Hence, $C_\ell C_{\ell'} = C_{\ell'}C_\ell$, $C_\ell^*C_{\ell'} = C_{\ell'}C_\ell^*$, $\ell, \ell' = 1,2,3$, $\ell \neq \ell'$, where C_1, C_2, C_3 are defined in (4.3), (4.7), (4.13), respectively.*

Proof. Without loss of generality, let $m_3 = 1 = m_2$ in Lemma 5.8, then $K_2(I_{n_2}\otimes K_1) = \left(I_{n_2}\otimes K_1\right)K_2$, which immediately implies $C_1C_2 = C_2C_1$, considering (1.5). Also $\left(I_{n_2}\otimes K_1\right)K_2^* = K_2^*\left(I_{n_2}\otimes K_1\right)$ holds, which immediately implies $C_1C_2^* = C_2^*C_1$. Yet, by Lemma 5.8, J_3 commutes with K_2, $I_{n_2}\otimes K_1$, K_2^*, $I_{n_2}\otimes K_1^*$, which implies $C_2C_3 = C_3C_2$, $C_1C_3 = C_3C_1$, $C_2^*C_3 = C_3C_2^*$, $C_1^*C_3 = C_3C_1^*$, considering (1.5). ∎

THEOREM 5.10. *K_3 in (4.13) is unitary. With X_i and Y_{ij} defined in (5.1) and (5.3b), respectively, K_3 satisfies*

$$K_3(Z_{ijk}\otimes Y_{ij}\otimes X_i) = \xi(\theta_{\mathbf{c},ij})\xi(k/n_3)(Z_{ijk}\otimes Y_{ij}\otimes X_i),$$

where

$$\theta_{\mathbf{c},ij} = \frac{1}{n_3}\left[\mathbf{k}\cdot\mathbf{c} - \frac{m_3}{n_2}j + \left(\frac{m_1}{n_1}\frac{m_3}{n_2} - \frac{m_2}{n_1}\right)i\right], \tag{5.4a}$$

$$Z_{ijk} = \left[1, \xi(\theta_{\mathbf{c},ij})\xi\left(\frac{k}{n_3}\right), \cdots, \xi((n_3-1)\theta_{\mathbf{c},ij})\xi\left(\frac{(n_3-1)k}{n_3}\right)\right]^\top, \tag{5.4b}$$

$$\mathbf{c} = \mathbf{a}_3 - \frac{m_3}{n_2}\mathbf{a}_2 + \left(\frac{m_1}{n_1}\frac{m_3}{n_2} - \frac{m_2}{n_1}\right)\mathbf{a}_1, \tag{5.4c}$$

for $i = 1, \cdots, n_1,\ j = 1, \cdots, n_2,\ k = 1, \cdots, n_3$.

Proof. By Lemma 5.8 and Lemma 5.3, we have $K_3^* K_3 = I_n$. Given i, j, by Theorem 5.6, K_2 has an eigenvector $v_{ij} = Y_{ij} \otimes X_i$, then by (1.5) and Theorem 5.2, $(\xi(\theta_{\mathbf{a}})\xi(i/n_1), v_{ij})$ is an eigenpair of $I_{n_2} \otimes K_1$. By Lemma 5.8, v_{ij} is also an eigenvector of $\xi(\mathbf{k}\cdot\mathbf{a}_3)J_3$, and the corresponding eigenvalue of $\xi(\mathbf{k}\cdot\mathbf{a}_3)J_3$ is

$$\xi(\mathbf{k}\cdot\mathbf{a}_3)\xi\left(-m_3\theta_{\mathbf{b},i}\right)\xi\left(-\frac{jm_3}{n_2}\right)\xi\left(-m_2\theta_{\mathbf{a}}\right)\xi\left(-\frac{im_2}{n_1}\right) = \xi(n_3\theta_{\mathbf{c},ij}),$$

where $\theta_{\mathbf{c},ij}$ is defined in (5.4a). Then by Lemma 5.3, the n_3-th root of $\xi(n_3\theta_{\mathbf{c},ij})$, which equals $\xi(\theta_{\mathbf{c},ij})\xi(k/n_3)$ with $k \in \{1, \cdots, n_3\}$, is an eigenvalue of K_3, and the corresponding eigenvector of K_3 is just $(Z_{ijk} \otimes Y_{ij} \otimes X_i)$ with Z_{ijk} in (5.4b). ∎

Remark 5.11. We have approximations $\eta_3 = m_3/n_2$, $\eta_2 = m_2/n_1$, $\eta_1 = m_1/n_1$ in (2.1), then the equality in (5.4c) holds ignoring the discretization error.

COROLLARY 5.12. *With* C_1, C_2, C_3 *defined in* (4.3)*,* (4.7)*,* (4.13)*, respectively, we have* $C_\ell C_\ell^* = C_\ell^* C_\ell$, $\ell = 1, 2, 3$.

Proof. By Theorems 5.2, 5.6, 5.10, K_1, K_2, K_3 are normal and commute with identity matrices with compatible sizes, hence C_1, C_2, C_3 are normal by Proposition 1.1. ∎

We summarize key results in this section for a nonzero $\mathbf{k}$ in (1.2) as follows:

$$C_\ell T = T\Lambda_\ell, \quad C_\ell^* T = T\overline{\Lambda_\ell}, \quad \ell = 1, 2, 3, \tag{5.5}$$

where

$$\begin{aligned}
\Lambda_1 &= \Lambda_{n_1} \otimes I_{n_2} \otimes I_{n_3}, \quad \Lambda_{n_1} = \mathbf{diag}\left(\xi(\theta_{\mathbf{a}})\xi([1:n_1]^\top/n_1) - 1\right)/\delta_x,\\
\Lambda_2 &= \oplus_{i=1}^{n_1}(\Lambda_{in_2} \otimes I_{n_3}), \quad \Lambda_{in_2} = \mathbf{diag}\left(\xi(\theta_{\mathbf{b},i})\xi([1:n_2]^\top/n_2) - 1\right)/\delta_y,\\
\Lambda_3 &= \oplus_{i=1}^{n_1}\left(\oplus_{j=1}^{n_2}\Lambda_{ijn_3}\right), \quad \Lambda_{ijn_3} = \mathbf{diag}\left(\xi(\theta_{\mathbf{c},ij})\xi([1:n_3]^\top/n_3) - 1\right)/\delta_z,
\end{aligned}$$

and

$$T(1:n,\, k + (j-1)n_3 + (i-1)n_2n_3) = (Z_{ijk} \otimes Y_{ij} \otimes X_i)/\sqrt{n}, \tag{5.6}$$

for $i = 1, \cdots, n_1,\ j = 1, \cdots, n_2,\ k = 1, \cdots, n_3$. By Theorem 5.10, all eigenvalues of K_3 are distinct, therefore, by Proposition 1.2, T defined in (5.6) is unitary.

Remark 5.13. In this work, eigen-decompositions in (5.5) are an immediate consequence of the fact that $\{C_\ell^*, C_\ell : \ell, \ell' = 1, 2, 3\}$ is a set of commutative matrices. This fact is compatible with the common sense that partial derivatives of a smooth field along any two of x-,y-,z-axes can be exchanged. In [14, 21], eigen-decompositions (5.5) have been derived for the SC and FCC lattices only. It becomes clear now that the formalism is the same for all Bravais lattices, though $\theta_{\mathbf{a}}$, $\theta_{\mathbf{b},i}$ and $\theta_{\mathbf{c},ij}$ depend on the specific lattice.

6. Range space of $\mathcal{C}$ and eigen-decomposition of $\mathcal{A}$. On the basis of the results in Sec. 5, we proceed to determine the range space and eigen-decomposition of $\mathcal{A} = \mathcal{C}^*\mathcal{C}$ analytically, without forming $\mathcal{C}^*\mathcal{C}$ explicitly.

From (4.20) and (5.5), we have

$$\mathcal{C} = (I_3 \otimes T)\mathbf{\Lambda}(I_3 \otimes T)^*, \tag{6.1}$$

$$\mathbf{\Lambda} = \begin{bmatrix} 0 & -T^*C_3T & T^*C_2T \\ T^*C_3T & 0 & -T^*C_1T \\ -T^*C_2T & T^*C_1T & 0 \end{bmatrix} = \begin{bmatrix} 0 & -\Lambda_3 & \Lambda_2 \\ \Lambda_3 & 0 & -\Lambda_1 \\ -\Lambda_2 & \Lambda_1 & 0 \end{bmatrix} = -\mathbf{\Lambda}^\top. \tag{6.2}$$

By doing a perfect shuffle $\mathbf{\Lambda}$ can be further transformed to a block diagonal matrix,

$$P = [e_1, e_{n+1}, e_{2n+1}, e_2, e_{n+2}, e_{2n+2}, \cdots, e_n, e_{2n}, e_{3n}] \in \mathbb{R}^{3n\times 3n}, \tag{6.3}$$

$$P^\top \mathbf{\Lambda} P = \oplus_{\ell=1}^n L_\ell, \quad L_\ell = -L_\ell^\top \in \mathbb{C}^{3\times 3}. \tag{6.4}$$

This means we can just deal with each block L_ℓ separately. Instead of the singular value decomposition of L_ℓ, the unitary congruence transformation of L_ℓ preserves the skew-symmetric structure and is very helpful in finding the range space of L_ℓ.

THEOREM 6.1. *Given a nonzero $g = [g_1, g_2, g_3]^\top \in \mathbb{C}^3$, it holds that*

$$L = \begin{bmatrix} 0 & -g_3 & g_2 \\ g_3 & 0 & -g_1 \\ -g_2 & g_1 & 0 \end{bmatrix} = \overline{V} \begin{bmatrix} 0 & 0 & 0 \\ 0 & 0 & -\beta \\ 0 & \beta & 0 \end{bmatrix} V^*, \quad \beta = ||g||,$$

where V is a Householder matrix satisfying $V^*g = \beta e_1$ and $VV^* = I_3$.

In Theorem 6.1, $V(:,1)$ is the nullspace of L, hence can be pruned. Then

$$L = \overline{\widehat{V}}(\beta\Gamma_2)\widehat{V}^*, \text{ where } \Gamma_2 = \begin{bmatrix} 0 & -1 \\ 1 & 0 \end{bmatrix}, \ \widehat{V} = V(:,[2,3]) \in \mathbb{C}^{3\times 2}, \ \widehat{V}^*\widehat{V} = I_2.$$

Similarly, for each $L_\ell = -L_\ell^\top \in \mathbb{C}^{3\times 3}$ in (6.4), we have

$$L_\ell = \overline{\widehat{V}}_\ell(\beta_\ell\Gamma_2)\widehat{V}_\ell^*, \quad \widehat{V}_\ell^*\widehat{V}_\ell = I_2, \tag{6.5}$$

where $\beta_\ell, \widehat{V}_\ell$ are defined in terms of entries of L_ℓ as in Theorem 6.1.

Consequently, $\mathbf{\Lambda}$ is unitarily congruent to a real quasi-diagonal skew-symmetric matrix and eigen-decomposition of $\mathcal{A}$ can be derived as follows.

THEOREM 6.2. *Given a nonzero $\mathbf{k}$ in (1.2), from (4.19), (4.20) and (6.1)–(6.5), we have*

$$(I_3 \otimes T)^*\mathcal{C}(I_3 \otimes T) = \overline{\mathcal{U}}_r\Gamma_r\mathcal{U}_r^*, \quad \mathcal{A} = \mathcal{C}^*\mathcal{C} = \mathcal{Q}_r\Lambda_r^2\mathcal{Q}_r^*, \tag{6.6}$$

where

$$\Gamma_r := \oplus_{\ell=1}^n(\beta_\ell\Gamma_2) \in \mathbb{R}^{2n\times 2n}, \quad \Lambda_r := \oplus_{\ell=1}^n(\beta_\ell I_2) \in \mathbb{R}^{2n\times 2n},$$
$$\mathcal{V}_r := \mathbf{blkdiag}\left(\widehat{V}_1, \widehat{V}_2, \cdots, \widehat{V}_n\right) \in \mathbb{C}^{3n\times 2n},$$
$$\mathcal{U}_r := P\mathcal{V}_r, \quad \mathcal{Q}_r := (I_3 \otimes T)\, P\mathcal{V}_r \text{ with } \mathcal{U}_r^*\mathcal{U}_r = I_{2n} = \mathcal{Q}_r^*\mathcal{Q}_r.$$

Proof. From (6.1), (6.4) and (6.5), we simply have

$$(I_3 \otimes T)^*\mathcal{C}(I_3 \otimes T) = \mathbf{\Lambda} = P\overline{\mathcal{V}}_r\Gamma_r\mathcal{V}_r^*P^\top = \overline{\mathcal{U}}_r\Gamma_r\mathcal{U}_r^*.$$

It is easily seen from (6.5) that $L_\ell^*L_\ell = \widehat{V}_\ell(\beta_\ell^2 I_2)\widehat{V}_\ell^*$. Then

$$\begin{aligned}\mathcal{A} = \mathcal{C}^*\mathcal{C} &= (I_3 \otimes T)\mathbf{\Lambda}^*\mathbf{\Lambda}(I_3 \otimes T)^* \\ &= ((I_3 \otimes T)P)\,\mathbf{blkdiag}(L_1^*L_1, L_2^*L_2, \cdots, L_n^*L_n)(P^\top(I_3 \otimes T)^*) \\ &= (I_3 \otimes T)P\mathcal{V}_r\Lambda_r^2\mathcal{V}_r^*P^\top(I_3 \otimes T)^* = \mathcal{Q}_r\Lambda_r^2\mathcal{Q}_r^*.\end{aligned}$$ ∎

Remark 6.3. When $\mathbf{k}$ vanishes, $\mathcal{Q}_r$ defined in Theorem 6.2 does not strictly span the range space of $\mathcal{A}$ and (7.1) below is not strictly NFSEP. But in practice, this makes little difference on the efficacy and efficiency of our numerical method discussed in next section. Therefore, we will not discuss this case specifically.

7. Eigensolver for NFSEP (7.1). Eventually, all previous derivations show that the nullspace free method proposed in [21] works for all Bravais lattices. With (6.6) in Theorem 6.2, the GEP (4.19) $\mathcal{A}E = \lambda\mathcal{B}E$ is transformed into the NFSEP:

$$\mathcal{A}_r\widehat{E} = \lambda\widehat{E}, \tag{7.1}$$

where

$$\mathcal{A}_r = \Lambda_r\mathcal{Q}_r^*\mathcal{B}^{-1}\mathcal{Q}_r\Lambda_r = \mathcal{A}_r^* > 0 \;\text{ and }\; \widehat{E} = \Lambda_r^{-1}\mathcal{Q}_r^*\mathcal{B}E.$$

Now the nullspace of GEP (4.19) has been completely deflated, therefore poses no threat to the desired solution of GEP (4.19).

To calculate a couple of smallest positive eigenvalues and associated eigenvectors of (7.1), a fast eigensolver was proposed in [21] originally for the SC and FCC lattices, and can also be similarly applied to all Bravais lattices. In brief, the invert Lanczos method is employed to calculate smallest few positive eigenvalues and associated eigenvectors of $\mathcal{A}_r$. The conjugate gradient (CG) method without preconditioner is employed to solve the linear system in each step of the invert Lanczos process, where the condition number of the coefficient matrix $\mathcal{Q}_r^*\mathcal{B}^{-1}\mathcal{Q}_r$ is bounded by that of $\mathcal{B}^{-1}$[21]. In the case of positive diagonal $\mathcal{B}$ with moderate condition number, the CG method turns out very appealing.

In the CG method, multiplying any column vector by $\mathcal{Q}_r^*\mathcal{B}^{-1}\mathcal{Q}_r$ is essentially reduced to Tq and T^*p except some diagonal scalings, where q and p are some intermediate vectors. Fortunately, we discover that the most expensive operations Tq and T^*p can be efficiently computed via Algorithm 1 and Algorithm 2 in [21], respectively, with slight modifications. In a nutshell, these two algorithms are just wrappers for the backward and forward FFTs, respectively, harnessing (1.4).

A preliminary MATLAB® implementation of our eigensolver has been developed into a software package called FAME [4], which stands for Fast Algorithm for Maxwell's Equations. The advanced functionality of FAME and other auxiliary components of FAME such as graphical user interface are still under development.

8. Numerical Experiments. To demonstrate the accuracy and efficiency of our framework, the band structure of the double gyroid PC [29] in the Body-Centered Cubic (BCC) lattice is calculated using FAME in MATLAB® R2017b environment. Key steps in our eigensolver are implemented calling functions **eigs**, **pcg**, **fft** and **ifft** of MATLAB®. In our calculation, the tolerance for convergence of **eigs** and **pcg**

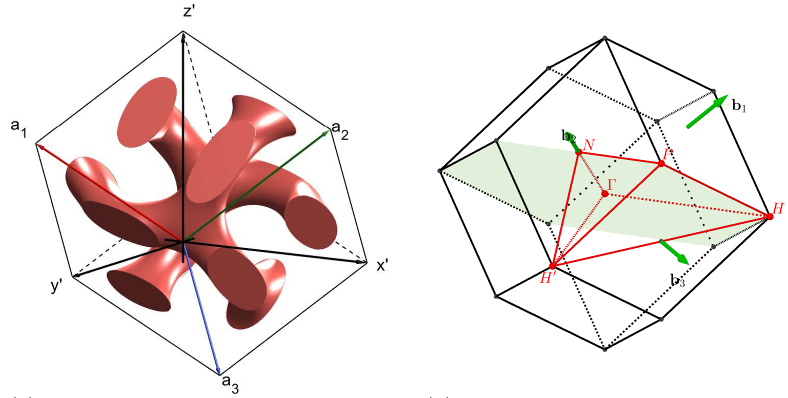

(a) The 3D physical cell of the BCC lattice and double gyroid structure.

(b) The Brillouin zone and its vertices of the BCC lattice.

FIG. 4. *Illustration of the PC in the BCC lattice and its Brillouin zone*

is set to 10^{-12} and 10^{-13}, respectively. All computations are performed on an Intel (R) Xeon (R) E5-2643 3.30GHz processor with 96 GB RAM in 64-bit IEEE double precision arithmetic.

In the prior orthogonal coordinate system, coordinates of lattice translation vectors $\mathbf{a}_1, \mathbf{a}_2, \mathbf{a}_3$ of the BCC lattice are

$$\mathbf{a}_1 = \widetilde{a}\,[-1;1;1]\,/2,\ \mathbf{a}_2 = \widetilde{a}\,[1;-1;1]\,/2,\ \mathbf{a}_3 = \widetilde{a}\,[1;1;-1]\,/2,$$

where $\widetilde{a}$ is the lattice constant. Reciprocal lattice vectors $[\mathbf{b}_1, \mathbf{b}_2, \mathbf{b}_3]$ are defined by $2\pi[\mathbf{a}_1, \mathbf{a}_2, \mathbf{a}_3]^{-\top}$. The coordinates of the vertices Γ, H, P, N, H' of the Brillouin zone (see Figure 4(b)) with respect to the basis $\mathbf{b}_1, \mathbf{b}_2, \mathbf{b}_3$ are

$$\Gamma = [0;0;0]\,,\ H = \left[\frac{1}{2};-\frac{1}{2};\frac{1}{2}\right],\ P = \left[\frac{1}{4};\frac{1}{4};\frac{1}{4}\right],\ N = \left[0;\frac{1}{2};0\right],\ H' = \left[-\frac{1}{2};\frac{1}{2};\frac{1}{2}\right].$$

In the prior orthogonal coordinate system, let $\mathbf{r} = [x';y';z']$. The double gyroid region in Figure 4(a) can be described by the set $\mathrm{DG} := \{\mathbf{r} \in \mathbb{R}^3 \,|\, f(\mathbf{r}) > 1.1\} \cup \{\mathbf{r} \in \mathbb{R}^3 \,|\, f(-\mathbf{r}) > 1.1\}$, where $f(\mathbf{r}) = \sin(2\pi[x',y',z']/a)\cos(2\pi[y';z';x']/a)$. For convenience, we set $a = 1$, $\varepsilon(\mathbf{r} \in \mathrm{DG}) = 16$, $\varepsilon(\mathbf{r} \notin \mathrm{DG}) = 1$. Ten smallest positive eigenvalues and associated eigenvectors of the NFSEP (7.1) are computed.

The band structure in Figure 5(a) does not show any discernible discrepancy with the one in [29], which partially evidences the accuracy of our method. Even the dimension of the NFSEP (7.1) is as large as $3,456,000$, it takes at most 7×10^3 seconds to finish the task at each **k**-point as shown in Figure 5(b) (1), which is acceptable in the case of serial implementation. More detailedly, in Figure 5(b) (2) the number of iterations in **eigs** versus **k** is plotted, where we can see that the invert Lanczos process converges in 60 to 170 steps for the ten target eigenpairs given **k**. In Figure 5(b) (3), the number of iterations in **pcg** without preconditioner versus **k** is plotted, where on average it takes 34 to 42 iterations to solve the linear system in one step of the invert Lanczos process. The overall efficiency of our eigensolver is impressive.

9. Conclusions. In a word, the major contribution we have made in the present work is the establishment of a complete and unified framework to solve the Maxwell Eigenvalue Problem for 3D isotropic photonic crystals in all 14 Bravais lattices. It is

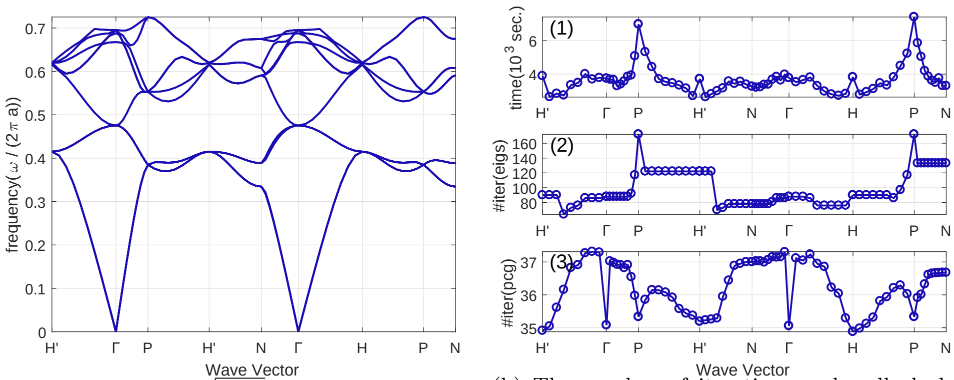

(a) $\omega = \sqrt{\lambda/\mu_0}$ versus $\mathbf{k}$

(b) The number of iterations and wall clock time

FIG. 5. *(a) The band structure of the double gyroid PC. (b)(1) The average number of iterations in* **pcg** *without preconditioner. (b)(2) The number of iterations in* **eigs***. (b)(3) The wall clock time spent on ten target eigenvalues.*

highlighted that our FAME is remarkably efficient. Compared with $\mathcal{O}(n^2)$ of other methods, the overall computational complexity of ours is $\mathcal{O}(n \log n)$, thanks to the feasibility of FFT algorithm in our framework, which is actually rooted in the eigen-decomposition of discrete partial derivative operators C_1, C_2, C_3 including the reformulated Bloch condition. Particularly, the novel discovery of the relations among unitary (block) companion matrices K_1, J_2, K_2, J_3 (see Corollary 5.5, Lemma 5.8) goes hand in hand with the hierarchical structure of the block companion matrices K_2, K_3 (see Lemma 5.3), which plays a central role in deriving important eigen-decompositions of C_1, C_2, C_3. With these apparatus, the whole process of derivations turns out uncluttered and reader-friendly. On the other hand, the fast convergence of our eigensolver is guaranteed by the novel nullspace free method that thoroughly removes the considerable nullspace of the discrete double-curl operator $\mathcal{A}$.

Extension of our present framework to 3D anisotropic photonic crystals is under investigation. Details of our package FAME and test of FAME in the high performance computing environment will be reported in near future.

Acknowledgments. T.-M. Huang was partially supported by the Ministry of Science and Technology (MoST) 105-2115-M-003-009-MY3, National Centre of Theoretical Sciences (NCTS) in Taiwan. T. Li was supported in parts by the NSFC 11471074. W.-W. Lin was partially supported by MoST 106-2628-M-009-004-, NCTS and ST Yau Centre in Taiwan. H. Tian was supported by MoST 107-2811-M-009-002-. Prof. So-Hsiang Chou is greatly appreciated for his valuable feedback and suggestion on this manuscript. Mr. Jyun-Wei Lin at National Chiao Tung University, who prepared many figures in this work, also deserves our gratitude.

REFERENCES

[1] *Bravais lattice.* https://en.wikipedia.org/wiki/Bravais_lattice.
[2] *Crystal systems and lattices.* http://aflowlib.duke.edu/users/egossett/lattice/lattice.html.
[3] *Eigenvectors of normal matrices.* https://proofwiki.org/wiki/Eigenvalues_of_Normal_Operator_have_Orthogonal_Eigenspaces.
[4] *Fast algorithms for maxwell's equations.* https://sites.google.com/g2.nctu.edu.tw/fame/home.

[5] *Kronecker product*. https://en.wikipedia.org/wiki/Kronecker_product.
[6] *Mathworks*. https://www.mathworks.com.
[7] *Normal matrix*. https://en.wikipedia.org/wiki/Normal_matrix.
[8] *Primitive cell*. https://en.wikipedia.org/wiki/Primitive_cell.
[9] A. Bossavit and J.-C. Verite, *A mixed fem-biem method to solve 3-D eddy-current problems*, IEEE Trans. Magnetics, 18 (1982), pp. 431–435.
[10] A. Chatterjee, L. C. Kempel, and J. L. Volakis, *Finite Element Method for Electromagnetics: Antennas, Microwave Circuits, and Scattering Applications*, IEEE Press, Piscataway, NJ, 1998.
[11] Z. Chen, Q. Du, and J. Zou, *Finite element methods with matching and nonmatching meshes for Maxwell equations with discontinuous coefficients*, SIAM J. Numer. Anal., 37 (2000), pp. 1542–1570.
[12] R. Chern, C. C. Chang, C.-C. Chang, and R. Hwang, *Large full band gaps for photonic crystals in two dimensions computed by an inverse method with multgrid acceleration*, Phys. Rev. E, 68 (2003), p. 26704.
[13] R.-L. Chern, C.-C. Chang, C.-C. Chang, and R.-R. Hwang, *Numerical study of three-dimensional photonic crystals with large band gaps*, J. Phys. Soc. Japan, 73 (2004), pp. 727–737.
[14] R.-L. Chern, H.-E. Hsieh, T.-M. Huang, W.-W. Lin, and W. Wang, *Singular value decompositions for single-curl operators in three-dimensional Maxwell's equations for complex media*, SIAM J. Matrix Anal. Appl., 36 (2015), pp. 203–224.
[15] J. E. J. Dennis, J. F. Traub, and W. R. P., *On the matrix polynomial, Lambda-matrix and block eigenvalue problems*, Tech. Report 71-109, December 1971. Available online at `https://ecommons.cornell.edu/handle/1813/5954`.
[16] D. C. Dobson and J. Pasciak, *Analysis for an algorithm for computing electromagnetic Bloch modes using Nedelec spaces*, Comp. Meth. Appl. Math., 1 (2001), pp. 138–153.
[17] S. Guo, F. Wu, S. Albin, and R. S. Rogowski, *Photonic band gap analysis using finite-difference frequency-domain method*, Opt. Express, 12 (2004), pp. 1741–1746.
[18] B. C. Gupta, C.-H. Kuo, and Z. Ye, *Propagation inhibition and localization of electromagnetic waves in two-dimensional random dielectric systems*, Phys. Rev. E, 69 (2004), p. 066615.
[19] M. Hano, *Finite-element analysis of dielectric-loaded waveguides*, IEEE. Trans. Microwave Theory Tech., 32 (1984), pp. 1275–1279.
[20] K. M. Ho, C.-T. Chan, and C. M. Soukoulis, *Existence of a photonic gap in periodic dielectric structures*, Phys. Rev. Lett., 65 (1990), p. 3152.
[21] T.-M. Huang, H.-E. Hsieh, W.-W. Lin, and W. Wang, *Eigendecomposition of the discrete double-curl operator with application to fast eigensolver for three dimensional photonic crystals*, SIAM J. Matrix Anal. Appl., 34 (2013), pp. 369–391.
[22] T.-M. Huang, H.-E. Hsieh, W.-W. Lin, and W. Wang, *Matrix representation of the double-curl operator for simulating three dimensional photonic crystals*, Math. Comput. Model., 58 (2013), pp. 379–392.
[23] J. Jin, *The finite element method in electromagnetics*, John Wiley, New York, NY, 2002.
[24] J. D. Joannopoulos, S. G. Johnson, J. N. Winn, and R. D. Meade, *Photonic Crystals: Molding the Flow of Light*, Princeton University Press, Princeton, NJ, 2008.
[25] J. D. Joannopoulos, P. R. Villeneuve, and S. Fan, *Photonic crystals: putting a new twist on light*, Nature, 386 (1997), p. 143.
[26] S. John, *Strong localization of photons in certain disordered dielectric superlattices*, Phys. Rev. Lett., 58 (1987), pp. 2486–2489.
[27] S. G. Johnson and J. D. Joannopoulos, *Block-iterative frequency-domain methods for Maxwell's equations in a planewave basis*, Opt. Express, 8 (2001), pp. 173–190.
[28] C. Kittel, *Introduction to solid state physics*, Wiley, New York, NY, 2005.
[29] L.-Z. Lu, L. Fu, J. D. Joannopoulos, and M. Soljačić, *Weyl points and line nodes in gyroid photonic crystals*, Nat. Photonics, 7 (2013), pp. 294–299.
[30] G. Mur and A. de Hoop, *A finite-element method for computing three-dimensional electromagnetic fields in inhomogeneous media*, IEEE Trans. Magnetics, 21 (1985), pp. 2188–2191.
[31] J.-C. Nédélec, *Mixed finite elements in* $\mathbb{R}^3$, Numer. Math., 35 (1980), pp. 315–341.
[32] J.-C. Nédélec, *A new class of mixed finite elements in* $\mathbb{R}^3$, Numer. Math., 50 (1986), pp. 57–81.
[33] P. A. Raviart and J. M. Thomas, *A mixed finite elemnt method for second order elliptic problems*, in Mathematical Aspects of the Finite Element Method, Lecture Notes in Math. 606, Springer-Verlag, New York, NY, 1977.
[34] M. C. Rechtsman, J. M. Zeuner, Y. Plotnik, Y. Lumer, D. Podolsky, F. Dreisow,

S. Nolte, M. Segev, and A. Szameit, *Photonic Floquet topological insulators*, Nature, 496 (2013), pp. 196–200.

[35] M. Reed and B. Simon, *Methods of modern mathematical physics*, in Analysis of Operators IV, Academic Press, San Diego, CA, 1978.

[36] K. Sakoda, *Optical properties of photonic crystals*, vol. 80, Springer Science & Business Media, 2004.

[37] V. Twersky, *Multiple scattering of radiation by an arbitrary configuration of parallel cylinders*, J. Acoust. Soc. Am., 24 (1952), pp. 42–46.

[38] W. S. Weiglhofer and A. Lakhtakia, *Introduction to Complex Mediums for Optics and Electromagnetics*, SPIE, Washington, DC, 2003.

[39] F. Xu, Y. Zhang, W. Hong, K. Wu, and T.-J. Cui, *Finite-difference frequency-domain algorithm for modeling guided-wave properties of substrate integrated waveguide*, IEEE Trans. Microwave Theo. Tech., 51 (2003), pp. 2221–2227.

[40] E. Yablonovitch, *Inhibited spontaneous emission in solid-state physics and electronics*, Phys. Rev. Lett., 58 (1987), pp. 2059–2062.

[41] K. Yasumoto, *Electromagnetic theory and applications for photonic crystals*, CRC Press, 2005.

[42] K. Yee, *Numerical solution of initial boundary value problems involving Maxwell's equations in isotropic media*, IEEE Trans. Antennas and Propagation, 14 (1966), pp. 302–307.

[43] C.-P. Yu and H.-C. Chang, *Compact finite-difference frequency-domain method for the analysis of two-dimensional photonic crystals*, Opt. Express, 12 (2004), pp. 1397–1408.

SUPPLEMENTARY MATERIALS: SOLVING THREE DIMENSIONAL MAXWELL EIGENVALUE PROBLEMS WITH FOURTEEN BRAVAIS LATTICES*

TSUNG-MING HUANG†, TIEXIANG LI‡, WEI-DE LI§, JIA-WEI LIN¶, WEN-WEI LIN ¶, AND HENG TIAN ¶

SM1. Derivation of Figure 2(b) and BC (3.3). It is best to visualize the investigation starting from Figure SM1(a), where we have $\phi_2, \phi_3 < \pi/2$, $\ell_2 > 0$, $a_3 \cos\phi_2 \geq a_2 \cos\phi_3$. Results of other possibilities will be discussed in SM2.

In Figure SM1(a), let $\square \mathrm{OR}_1\mathrm{R}_2\mathrm{R}_3$ be the bottom surface of $\mathbb{D}$, and $\square \mathrm{R}_4\mathrm{R}_5\mathrm{R}_6\mathrm{R}_7$ be the image of the top surface of $\mathbb{D}$ under $\mathcal{T}_{-\mathbf{a}_3}$, which contains the origin in this case. We naturally have the 2D oblique coordinate system with $\mathbf{a}_1$-,$\mathbf{a}_2$-axes. With slight abuse of notation, I,II,III,IV denote four patches of the $\square \mathrm{R}_4\mathrm{R}_5\mathrm{R}_6\mathrm{R}_7$, located in the first, second, third, fourth quadrant, respectively, of this oblique coordinate system. Our goal is to map $\square \mathrm{R}_4\mathrm{R}_5\mathrm{R}_6\mathrm{R}_7$ to $\square \mathrm{OR}_1\mathrm{R}_2\mathrm{R}_3$, respecting the periodicity along $\mathbf{a}_1, \mathbf{a}_2$.

We have the 2D physical cell generated by $\mathbf{a}_1, \mathbf{a}_2$, *i.e.*, the set $\{\alpha\mathbf{a}_1 + \beta\mathbf{a}_2 : \alpha, \beta \in [0, 1)\}$, and its periodic images under $\mathcal{T}_{\mathbf{a}_1}, \mathcal{T}_{\mathbf{a}_2}$ which fill up the whole plane, *i.e.*, the set $\{\alpha\mathbf{a}_1 + \beta\mathbf{a}_2 : \alpha, \beta \in \mathbb{R}\}$. Due to the periodicity, it is best to narrow our attention to the 2D physical cell. The rule is that whenever a point is outside the 2D physical cell, *i.e.*, $\alpha, \beta \notin [0, 1)$, we evaluate its image within the 2D physical cell under the modulo operation

$$\alpha\mathbf{a}_1 + \beta\mathbf{a}_2 \equiv (\alpha - \mathbf{floor}(\alpha))\,\mathbf{a}_1 + (\beta - \mathbf{floor}(\beta))\,\mathbf{a}_2 \mod \mathbf{a}_1, \mathbf{a}_2.$$

For example, with respect to the nonorthogonal basis $\mathbf{a}_1, \mathbf{a}_2$ coordinates of points in patch III satisfy $\alpha, \beta \in [-1, 0)$, then due to

$$\alpha\mathbf{a}_1 + \beta\mathbf{a}_2 \equiv (1+\alpha)\mathbf{a}_1 + (1+\beta)\mathbf{a}_2 = \mathcal{T}_{\mathbf{a}_1}\mathcal{T}_{\mathbf{a}_2}(\alpha\mathbf{a}_1 + \beta\mathbf{a}_2) \mod \mathbf{a}_1, \mathbf{a}_2,$$

patch III is mapped to its counterpart in the 2D physical cell shown in Figure SM1(b). Other patches are similarly relocated.

As shown in Figure SM1(c), it is easy to map the 2D physical cell to $\square \mathrm{OR}_1\mathrm{R}_2\mathrm{R}_3$, which is realized if triangle Ω_2 in the 2D physical cell is mapped to its counterpart in the second quadrant.

Finally in Figure SM1(d), by composition of operations in Figure SM1(b) and Figure SM1(c), $\square \mathrm{R}_4\mathrm{R}_5\mathrm{R}_6\mathrm{R}_7$ is mapped to $\square \mathrm{OR}_1\mathrm{R}_2\mathrm{R}_3$.

In summary, there should be four patches within $\square \mathrm{OR}_1\mathrm{R}_2\mathrm{R}_3$, namely, $(\mathrm{II} \cap \Omega_2) \cup \mathrm{I}$, $\mathrm{II} \cap \Omega_1$, $\mathrm{III} \cap \Omega_1$, $(\mathrm{III} \cap \Omega_2) \cup \mathrm{IV}$. The linear mapping of each patch to $\square \mathrm{R}_4\mathrm{R}_5\mathrm{R}_6\mathrm{R}_7$ is $\mathcal{T}_0$, $\mathcal{T}_{-\mathbf{a}_1}$, $\mathcal{T}_{-\mathbf{a}_1-\mathbf{a}_2}$, $\mathcal{T}_{-\mathbf{a}_2}$, respectively, comparing Figure SM1(a) with Figure SM1(d).

*Submitted to the editors August 02, 2018.

Funding: This work was funded by MoST 105-2115-M-003-009-MY3, NSFC 11471074, MoST 106-2628-M-009-004-, MoST 107-2811-M-009-002-.

†Department of Mathematics, National Taiwan Normal University, Taipei, 116, Taiwan, (min@ntnu.edu.tw).

‡School of Mathematics, Southeast University, Nanjing 211189, People's Republic of China, (txli@seu.edu.cn).

§Department of Mathematics, National Tsing-Hua University, Hsinchu 300, Taiwan, (weideli@gapp.nthu.edu.tw).

¶Department of Applied Mathematics, National Chiao Tung University, Hsinchu 300, Taiwan, (jiawei.am05g@g2.nctu.edu.tw, wwlin@math.nctu.edu.tw, tianheng@nctu.edu.tw).

Furthermore, comparing Figure SM1(d) and Figure 2(b) we identify four patches Figure SM1(d) with four patches within $\square \mathrm{OR}_1\mathrm{R}_2\mathrm{R}_3$ in Figure 2(b), namely

- $(\mathrm{II} \cap \Omega_2) \cup \mathrm{I} \mapsto \mathrm{I}, \quad \mathrm{II} \cap \Omega_1 \mapsto \mathrm{II}$,
- $\mathrm{III} \cap \Omega_1 \mapsto \mathrm{III}, \quad (\mathrm{III} \cap \Omega_2) \cup \mathrm{IV} \mapsto \mathrm{IV}$.

SM2. J_2 and J_3 in the triclinic lattice. Recall that $\tilde{\mathbf{a}}_1, \tilde{\mathbf{a}}_2, \tilde{\mathbf{a}}_3$ are assumed to be $\mathbf{a}_1, \mathbf{a}_2, \mathbf{a}_3$ and that $\mathbf{a}_3^{\perp}$ is the projection of $\mathbf{a}_3$ onto the xy-plane in the orthogonal coordinate system with x-,y-,z-axes. The four quadrants in the xy-plane partitioned by x-,y-axes are denoted by $\mathfrak{I}, \mathfrak{II}, \mathfrak{III}, \mathfrak{IV}$. As illustrated in Figure SM2, SM3, SM4 and SM5, we classify the triclinic lattice into four categories according to the quadrant in which $\mathbf{a}_3^{\perp}$ is located, and further divide each category into four subcategories according to the quadrant in which $\mathbf{a}_2$ is located and the first coordinates of $\mathbf{a}_1, \mathbf{a}_2, \mathbf{a}_3$, *i.e.*, $\mathbf{a}_1(1), \mathbf{a}_2(1), \mathbf{a}_3(1)$. We will reformulate the BC (1.2) for each subcategory.

The image of the top surface of $\mathbb{D}$ under $\mathcal{T}_{-\mathbf{a}_3}$ is partitioned into $\widetilde{\mathrm{I}}$, $\widetilde{\mathrm{II}}$, $\widetilde{\mathrm{III}}$, $\widetilde{\mathrm{IV}}$, while the bottom surface of $\mathbb{D}$ is accordingly partitioned into I, II, III, IV. It is clear that there is always one patch in the former which overlaps with another patch in the latter and is associated with the identity mapping $\mathcal{T}_0$. Following the same reasoning in SM1, we present the results as follows. Let $\mathbf{x} = (x, y, 0) \in \mathbb{D}$ be the point in the bottom surface of $\mathbb{D}$, and recall that $\xi(\theta) := \exp(\imath 2\pi\theta)$.

- Case (1-i): $\mathbf{a}_3^{\perp} \in \mathfrak{I},\ \mathbf{a}_2 \in \mathfrak{I},\ \mathbf{a}_2(1) \leq \mathbf{a}_3(1)$,

$$\boldsymbol{E}(\mathbf{x}) = \begin{cases} \boldsymbol{E}(\mathbf{x}), & \text{if } \mathbf{x} \in \mathrm{I} \\ \xi(\mathbf{k}\cdot\mathbf{a}_1)\boldsymbol{E}(\mathbf{x}-\mathbf{a}_1), & \text{if } \mathbf{x} \in \mathrm{II} \\ \xi(\mathbf{k}\cdot(\mathbf{a}_1+\mathbf{a}_2))\boldsymbol{E}(\mathbf{x}-\mathbf{a}_1-\mathbf{a}_2), & \text{if } \mathbf{x} \in \mathrm{III} \\ \xi(\mathbf{k}\cdot\mathbf{a}_2)\boldsymbol{E}(\mathbf{x}-\mathbf{a}_2), & \text{if } \mathbf{x} \in \mathrm{IV}. \end{cases} \tag{SM2.1}$$

- Case (1-ii): $\mathbf{a}_3^{\perp} \in \mathfrak{I},\ \mathbf{a}_2 \in \mathfrak{I},\ \mathbf{a}_2(1) > \mathbf{a}_3(1)$,

$$\boldsymbol{E}(\mathbf{x}) = \begin{cases} \boldsymbol{E}(\mathbf{x}), & \text{if } \mathbf{x} \in \mathrm{I} \\ \xi(\mathbf{k}\cdot\mathbf{a}_1)\boldsymbol{E}(\mathbf{x}-\mathbf{a}_1), & \text{if } \mathbf{x} \in \mathrm{II} \\ \xi(\mathbf{k}\cdot\mathbf{a}_2)\boldsymbol{E}(\mathbf{x}-\mathbf{a}_2), & \text{if } \mathbf{x} \in \mathrm{III} \\ \xi(\mathbf{k}\cdot(-\mathbf{a}_1+\mathbf{a}_2))\boldsymbol{E}(\mathbf{x}+\mathbf{a}_1-\mathbf{a}_2), & \text{if } \mathbf{x} \in \mathrm{IV}. \end{cases} \tag{SM2.2}$$

- Case (1-iii): $\mathbf{a}_3^{\perp} \in \mathfrak{I},\ \mathbf{a}_2 \in \mathfrak{II},\ -\mathbf{a}_2(1) \leq \mathbf{a}_1(1) - \mathbf{a}_3(1)$,

$$\boldsymbol{E}(\mathbf{x}) = \begin{cases} \boldsymbol{E}(\mathbf{x}), & \text{if } \mathbf{x} \in \mathrm{I} \\ \xi(\mathbf{k}\cdot\mathbf{a}_1)\boldsymbol{E}(\mathbf{x}-\mathbf{a}_1), & \text{if } \mathbf{x} \in \mathrm{II} \\ \xi(\mathbf{k}\cdot(\mathbf{a}_1+\mathbf{a}_2))\boldsymbol{E}(\mathbf{x}-\mathbf{a}_1-\mathbf{a}_2), & \text{if } \mathbf{x} \in \mathrm{III} \\ \xi(\mathbf{k}\cdot\mathbf{a}_2)\boldsymbol{E}(\mathbf{x}-\mathbf{a}_2), & \text{if } \mathbf{x} \in \mathrm{IV}. \end{cases} \tag{SM2.3}$$

- Case (1-iv): $\mathbf{a}_3^{\perp} \in \mathfrak{I},\ \mathbf{a}_2 \in \mathfrak{II},\ -\mathbf{a}_2(1) > \mathbf{a}_1(1) - \mathbf{a}_3(1)$,

$$\boldsymbol{E}(\mathbf{x}) = \begin{cases} \boldsymbol{E}(\mathbf{x}), & \text{if } \mathbf{x} \in \mathrm{I} \\ \xi(\mathbf{k}\cdot\mathbf{a}_1)\boldsymbol{E}(\mathbf{x}-\mathbf{a}_1), & \text{if } \mathbf{x} \in \mathrm{II} \\ \xi(\mathbf{k}\cdot(2\mathbf{a}_1+\mathbf{a}_2))\boldsymbol{E}(\mathbf{x}-2\mathbf{a}_1-\mathbf{a}_2), & \text{if } \mathbf{x} \in \mathrm{III} \\ \xi(\mathbf{k}\cdot(\mathbf{a}_1+\mathbf{a}_2))\boldsymbol{E}(\mathbf{x}-\mathbf{a}_1-\mathbf{a}_2), & \text{if } \mathbf{x} \in \mathrm{IV}. \end{cases} \tag{SM2.4}$$

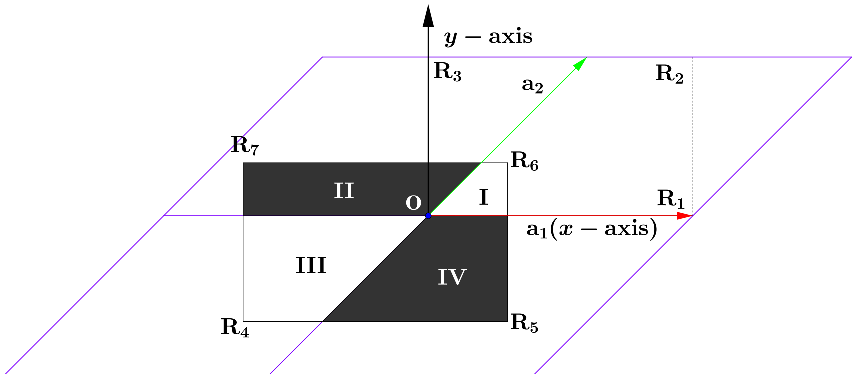

(a) $\square R_4R_5R_6R_7$ is partitioned into 4 patches by $\mathbf{a}_1$-,$\mathbf{a}_2$-axes.

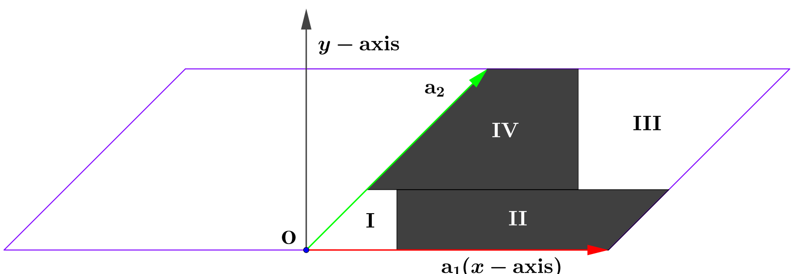

(b) All 4 patches are relocated to the first quadrant.

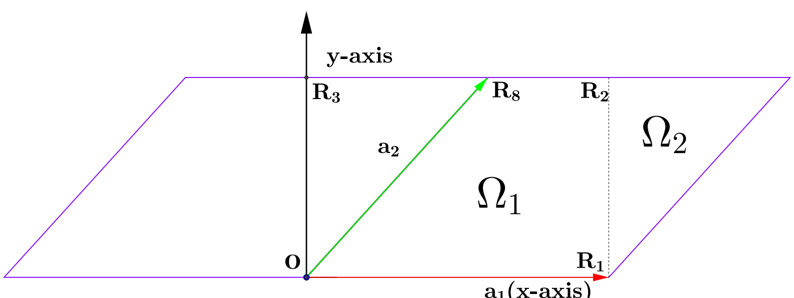

(c) The 2D physical cell is mapped to $\square OR_1R_2R_3$ if triangle Ω_2 is relocated to triangle OR_8R_3.

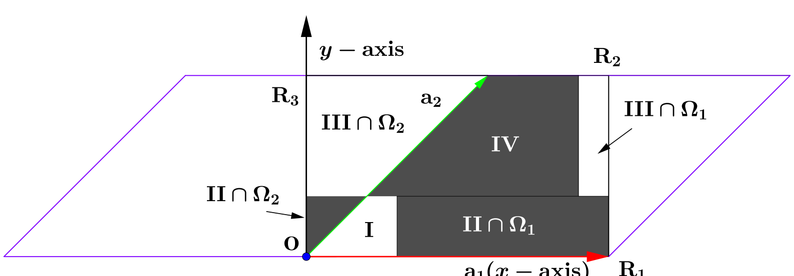

(d) $\square R_4R_5R_6R_7$ is finally mapped to $\square OR_1R_2R_3$ if $II \cap \Omega_2$ and $III \cap \Omega_2$ are relocated to the second quadrant.

FIG. SM1. *Derivation of the BC (3.3) along the z-axis.*

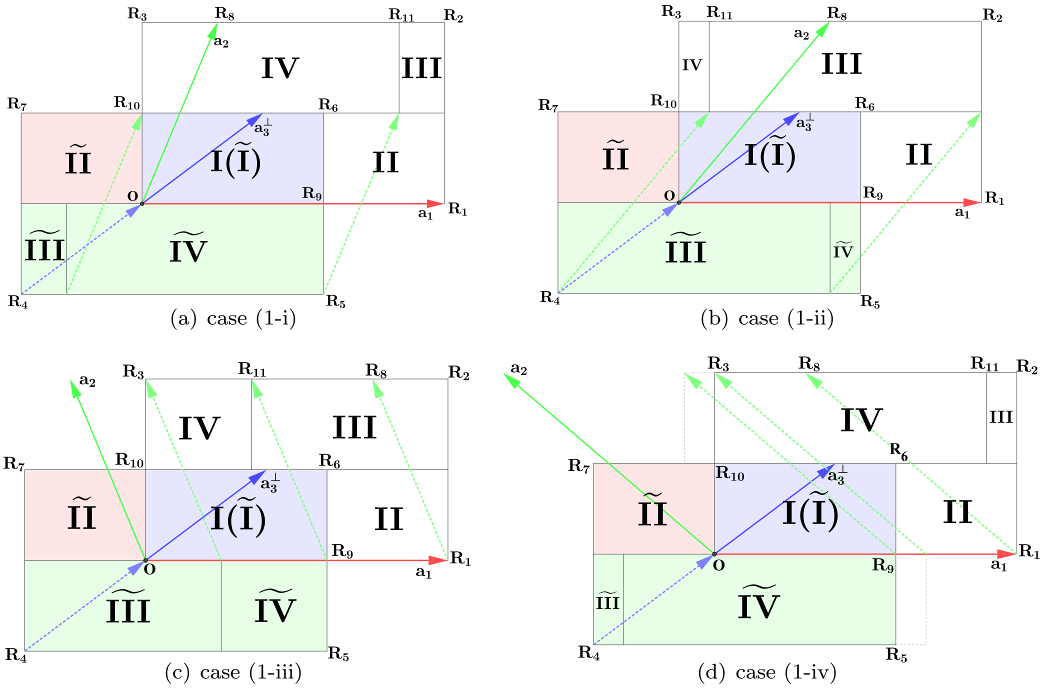

FIG. SM2. *Four subcategories of the first category where* $\mathbf{a}_3^{\perp} \in \mathfrak{I}$.

- Case (2-i): $\mathbf{a}_3^{\perp} \in \mathfrak{I}\mathfrak{I}$, $\mathbf{a}_2 \in \mathfrak{I}$, $\mathbf{a}_2(1) \leq \mathbf{a}_1(1) + \mathbf{a}_3(1)$,

$$\boldsymbol{E}(\mathbf{x}) = \begin{cases} \xi(-\mathbf{k}\cdot\mathbf{a}_1)\boldsymbol{E}(\mathbf{x}+\mathbf{a}_1), & \text{if } \mathbf{x} \in \mathrm{I} \\ \boldsymbol{E}(\mathbf{x}), & \text{if } \mathbf{x} \in \mathrm{II} \\ \xi(\mathbf{k}\cdot\mathbf{a}_2)\boldsymbol{E}(\mathbf{x}-\mathbf{a}_2), & \text{if } \mathbf{x} \in \mathrm{III} \\ \xi(\mathbf{k}\cdot(-\mathbf{a}_1+\mathbf{a}_2))\boldsymbol{E}(\mathbf{x}+\mathbf{a}_1-\mathbf{a}_2), & \text{if } \mathbf{x} \in \mathrm{IV}. \end{cases} \tag{SM2.5}$$

- Case (2-ii): $\mathbf{a}_3^{\perp} \in \mathfrak{I}\mathfrak{I}$, $\mathbf{a}_2 \in \mathfrak{I}$, $\mathbf{a}_2(1) > \mathbf{a}_1(1) + \mathbf{a}_3(1)$,

$$\boldsymbol{E}(\mathbf{x}) = \begin{cases} \xi(-\mathbf{k}\cdot\mathbf{a}_1)\boldsymbol{E}(\mathbf{x}+\mathbf{a}_1), & \text{if } \mathbf{x} \in \mathrm{I} \\ \boldsymbol{E}(\mathbf{x}), & \text{if } \mathbf{x} \in \mathrm{II} \\ \xi(\mathbf{k}\cdot(-\mathbf{a}_1+\mathbf{a}_2))\boldsymbol{E}(\mathbf{x}+\mathbf{a}_1-\mathbf{a}_2), & \text{if } \mathbf{x} \in \mathrm{III} \\ \xi(\mathbf{k}\cdot(-2\mathbf{a}_1+\mathbf{a}_2))\boldsymbol{E}(\mathbf{x}+2\mathbf{a}_1-\mathbf{a}_2), & \text{if } \mathbf{x} \in \mathrm{IV}. \end{cases} \tag{SM2.6}$$

- Case (2-iii): $\mathbf{a}_3^{\perp} \in \mathfrak{I}\mathfrak{I}$, $\mathbf{a}_2 \in \mathfrak{I}\mathfrak{I}$, $-\mathbf{a}_2(1) \leq -\mathbf{a}_3(1)$,

$$\boldsymbol{E}(\mathbf{x}) = \begin{cases} \xi(-\mathbf{k}\cdot\mathbf{a}_1)\boldsymbol{E}(\mathbf{x}+\mathbf{a}_1), & \text{if } \mathbf{x} \in \mathrm{I} \\ \boldsymbol{E}(\mathbf{x}), & \text{if } \mathbf{x} \in \mathrm{II} \\ \xi(\mathbf{k}\cdot\mathbf{a}_2)\boldsymbol{E}(\mathbf{x}-\mathbf{a}_2), & \text{if } \mathbf{x} \in \mathrm{III} \\ \xi(\mathbf{k}\cdot(-\mathbf{a}_1+\mathbf{a}_2))\boldsymbol{E}(\mathbf{x}+\mathbf{a}_1-\mathbf{a}_2), & \text{if } \mathbf{x} \in \mathrm{IV}. \end{cases} \tag{SM2.7}$$

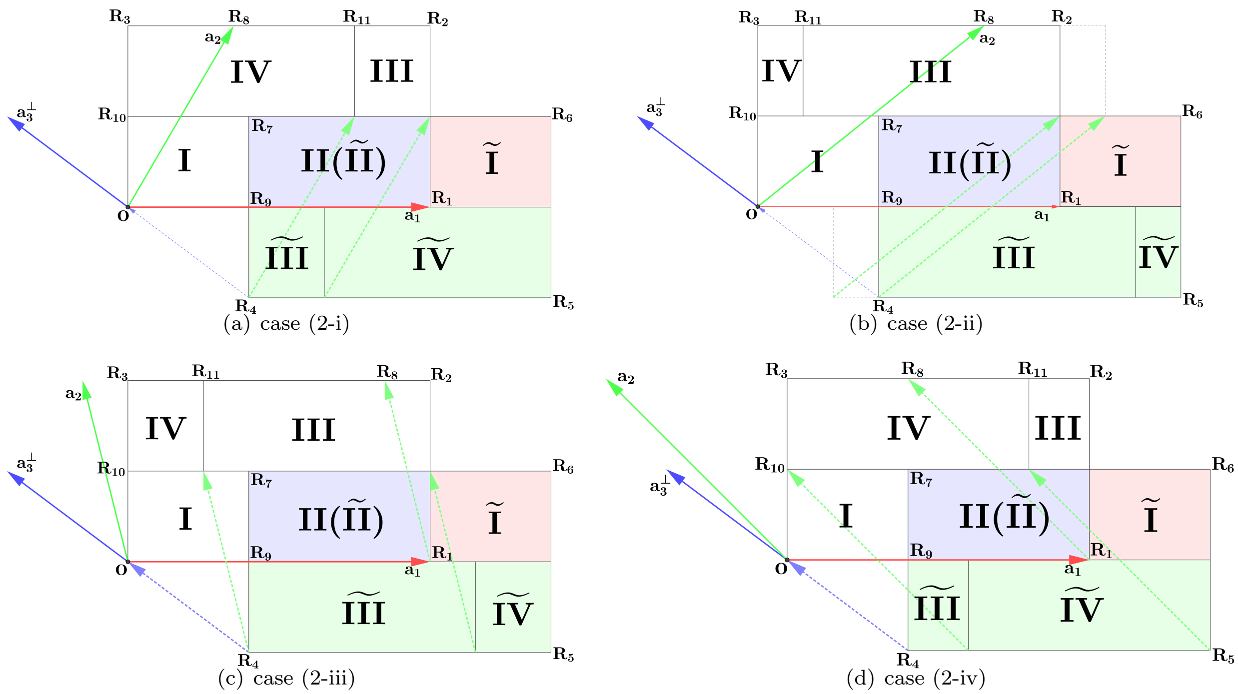

(a) case (2-i) (b) case (2-ii) (c) case (2-iii) (d) case (2-iv)

FIG. SM3. *Four subcategories of the second category where* $\mathbf{a}_3^{\perp} \in \mathfrak{I}\mathfrak{I}$.

- Case (2-iv): $\mathbf{a}_3^{\perp} \in \mathfrak{I}\mathfrak{I},\ \mathbf{a}_2 \in \mathfrak{I}\mathfrak{I},\ -\mathbf{a}_2(1) > -\mathbf{a}_3(1)$,

$$\boldsymbol{E}(\mathbf{x}) = \begin{cases} \xi(-\mathbf{k}\cdot\mathbf{a}_1)\boldsymbol{E}(\mathbf{x}+\mathbf{a}_1), & \text{if } \mathbf{x} \in \mathrm{I} \\ \boldsymbol{E}(\mathbf{x}), & \text{if } \mathbf{x} \in \mathrm{II} \\ \xi(\mathbf{k}\cdot(\mathbf{a}_1+\mathbf{a}_2))\boldsymbol{E}(\mathbf{x}-\mathbf{a}_1-\mathbf{a}_2), & \text{if } \mathbf{x} \in \mathrm{III} \\ \xi(\mathbf{k}\cdot\mathbf{a}_2)\boldsymbol{E}(\mathbf{x}-\mathbf{a}_2), & \text{if } \mathbf{x} \in \mathrm{IV}. \end{cases} \tag{SM2.8}$$

- Case (3-i): $\mathbf{a}_3^{\perp} \in \mathfrak{I}\mathfrak{I}\mathfrak{I},\ \mathbf{a}_2 \in \mathfrak{I},\ \mathbf{a}_2(1) \le -\mathbf{a}_3(1)$,

$$\boldsymbol{E}(\mathbf{x}) = \begin{cases} \xi(-\mathbf{k}\cdot(\mathbf{a}_1+\mathbf{a}_2))\boldsymbol{E}(\mathbf{x}+\mathbf{a}_1+\mathbf{a}_2), & \text{if } \mathbf{x} \in \mathrm{I} \\ \xi(-\mathbf{k}\cdot\mathbf{a}_2)\boldsymbol{E}(\mathbf{x}+\mathbf{a}_2), & \text{if } \mathbf{x} \in \mathrm{II} \\ \boldsymbol{E}(\mathbf{x}), & \text{if } \mathbf{x} \in \mathrm{III} \\ \xi(-\mathbf{k}\cdot\mathbf{a}_1)\boldsymbol{E}(\mathbf{x}+\mathbf{a}_1), & \text{if } \mathbf{x} \in \mathrm{IV}. \end{cases} \tag{SM2.9}$$

- Case (3-ii): $\mathbf{a}_3^{\perp} \in \mathfrak{I}\mathfrak{I}\mathfrak{I},\ \mathbf{a}_2 \in \mathfrak{I},\ \mathbf{a}_2(1) > -\mathbf{a}_3(1)$,

$$\boldsymbol{E}(\mathbf{x}) = \begin{cases} \xi(-\mathbf{k}\cdot\mathbf{a}_2)\boldsymbol{E}(\mathbf{x}+\mathbf{a}_2), & \text{if } \mathbf{x} \in \mathrm{I} \\ \xi(\mathbf{k}\cdot(\mathbf{a}_1-\mathbf{a}_2))\boldsymbol{E}(\mathbf{x}-\mathbf{a}_1+\mathbf{a}_2), & \text{if } \mathbf{x} \in \mathrm{II} \\ \boldsymbol{E}(\mathbf{x}), & \text{if } \mathbf{x} \in \mathrm{III} \\ \xi(-\mathbf{k}\cdot\mathbf{a}_1)\boldsymbol{E}(\mathbf{x}+\mathbf{a}_1), & \text{if } \mathbf{x} \in \mathrm{IV}. \end{cases} \tag{SM2.10}$$

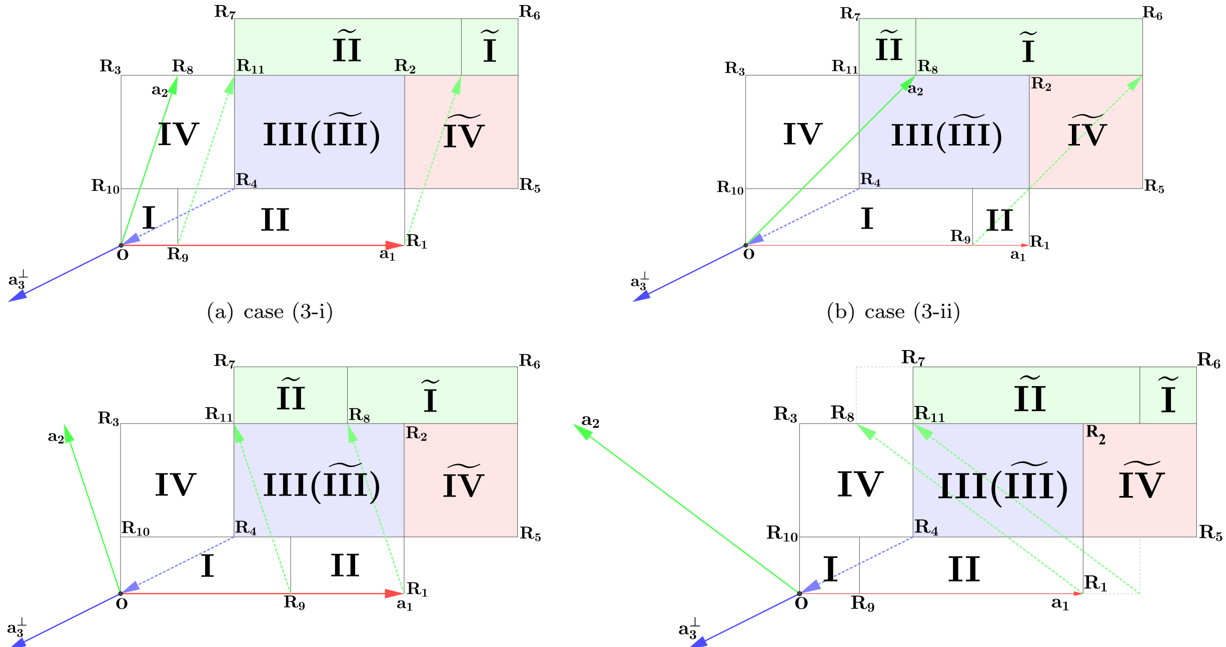

(a) case (3-i) (b) case (3-ii)

(c) case (3-iii) (d) case (3-iv)

FIG. SM4. *Four subcategories of the third category where* $\mathbf{a}_3^\perp \in \mathfrak{III}$.

- Case (3-iii): $\mathbf{a}_3^\perp \in \mathfrak{III},\ \mathbf{a}_2 \in \mathfrak{II},\ -\mathbf{a}_2(1) \leq \mathbf{a}_1(1) + \mathbf{a}_3(1)$,

$$\boldsymbol{E}(\mathbf{x}) = \begin{cases} \xi(-\mathbf{k}\cdot(\mathbf{a}_1+\mathbf{a}_2))\boldsymbol{E}(\mathbf{x}+\mathbf{a}_1+\mathbf{a}_2), & \text{if } \mathbf{x} \in \text{I} \\ \xi(-\mathbf{k}\cdot\mathbf{a}_2)\boldsymbol{E}(\mathbf{x}+\mathbf{a}_2), & \text{if } \mathbf{x} \in \text{II} \\ \boldsymbol{E}(\mathbf{x}), & \text{if } \mathbf{x} \in \text{III} \\ \xi(-\mathbf{k}\cdot\mathbf{a}_1)\boldsymbol{E}(\mathbf{x}+\mathbf{a}_1), & \text{if } \mathbf{x} \in \text{IV}. \end{cases} \tag{SM2.11}$$

- Case (3-iv): $\mathbf{a}_3^\perp \in \mathfrak{III},\ \mathbf{a}_2 \in \mathfrak{II},\ -\mathbf{a}_2(1) > \mathbf{a}_1(1) + \mathbf{a}_3(1)$,

$$\boldsymbol{E}(\mathbf{x}) = \begin{cases} \xi(-\mathbf{k}\cdot(2\mathbf{a}_1+\mathbf{a}_2))\boldsymbol{E}(\mathbf{x}+2\mathbf{a}_1+\mathbf{a}_2), & \text{if } \mathbf{x} \in \text{I} \\ \xi(-\mathbf{k}\cdot(\mathbf{a}_1+\mathbf{a}_2))\boldsymbol{E}(\mathbf{x}+\mathbf{a}_1+\mathbf{a}_2), & \text{if } \mathbf{x} \in \text{II} \\ \boldsymbol{E}(\mathbf{x}), & \text{if } \mathbf{x} \in \text{III} \\ \xi(-\mathbf{k}\cdot\mathbf{a}_1)\boldsymbol{E}(\mathbf{x}+\mathbf{a}_1), & \text{if } \mathbf{x} \in \text{IV}. \end{cases} \tag{SM2.12}$$

- Case (4-i): $\mathbf{a}_3^\perp \in \mathfrak{IV},\ \mathbf{a}_2 \in \mathfrak{I},\ \mathbf{a}_2(1) \leq \mathbf{a}_1(1) - \mathbf{a}_3(1)$,

$$\boldsymbol{E}(\mathbf{x}) = \begin{cases} \xi(-\mathbf{k}\cdot\mathbf{a}_2)\boldsymbol{E}(\mathbf{x}+\mathbf{a}_2), & \text{if } \mathbf{x} \in \text{I} \\ \xi(\mathbf{k}\cdot(\mathbf{a}_1-\mathbf{a}_2))\boldsymbol{E}(\mathbf{x}-\mathbf{a}_1+\mathbf{a}_2), & \text{if } \mathbf{x} \in \text{II} \\ \xi(\mathbf{k}\cdot\mathbf{a}_1)\boldsymbol{E}(\mathbf{x}-\mathbf{a}_1), & \text{if } \mathbf{x} \in \text{III} \\ \boldsymbol{E}(\mathbf{x}), & \text{if } \mathbf{x} \in \text{IV}. \end{cases} \tag{SM2.13}$$

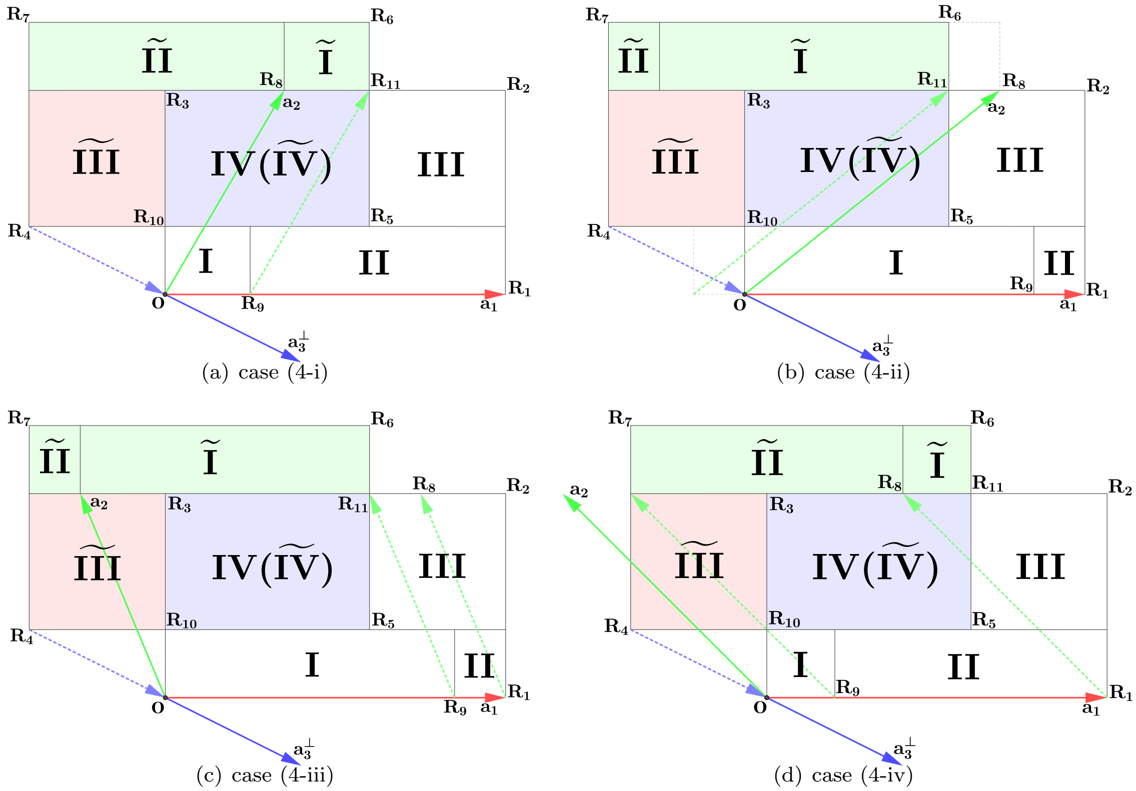

FIG. SM5. *Four subcategories of the fourth category where* $\mathbf{a}_3^\perp \in \mathfrak{IV}$.

- Case (4-ii): $\mathbf{a}_3^\perp \in \mathfrak{IV},\ \mathbf{a}_2 \in \mathfrak{I},\ \mathbf{a}_2(1) > \mathbf{a}_1(1) - \mathbf{a}_3(1)$,

$$\boldsymbol{E}(\mathbf{x}) = \begin{cases} \xi(\mathbf{k}\cdot(\mathbf{a}_1 - \mathbf{a}_2))\boldsymbol{E}(\mathbf{x} - \mathbf{a}_1 + \mathbf{a}_2), & \text{if } \mathbf{x} \in \mathrm{I} \\ \xi(\mathbf{k}\cdot(2\mathbf{a}_1 - \mathbf{a}_2))\boldsymbol{E}(\mathbf{x} - 2\mathbf{a}_1 + \mathbf{a}_2), & \text{if } \mathbf{x} \in \mathrm{II} \\ \xi(\mathbf{k}\cdot\mathbf{a}_1)\boldsymbol{E}(\mathbf{x} - \mathbf{a}_1), & \text{if } \mathbf{x} \in \mathrm{III} \\ \boldsymbol{E}(\mathbf{x}), & \text{if } \mathbf{x} \in \mathrm{IV}. \end{cases} \tag{SM2.14}$$

- Case (4-iii): $\mathbf{a}_3^\perp \in \mathfrak{IV},\ \mathbf{a}_2 \in \mathfrak{II},\ -\mathbf{a}_2(1) \leq \mathbf{a}_3(1)$,

$$\boldsymbol{E}(\mathbf{x}) = \begin{cases} \xi(-\mathbf{k}\cdot\mathbf{a}_2)\boldsymbol{E}(\mathbf{x} + \mathbf{a}_2), & \text{if } \mathbf{x} \in \mathrm{I} \\ \xi(\mathbf{k}\cdot(\mathbf{a}_1 - \mathbf{a}_2))\boldsymbol{E}(\mathbf{x} - \mathbf{a}_1 + \mathbf{a}_2), & \text{if } \mathbf{x} \in \mathrm{II} \\ \xi(\mathbf{k}\cdot\mathbf{a}_1)\boldsymbol{E}(\mathbf{x} - \mathbf{a}_1), & \text{if } \mathbf{x} \in \mathrm{III} \\ \boldsymbol{E}(\mathbf{x}), & \text{if } \mathbf{x} \in \mathrm{IV}. \end{cases} \tag{SM2.15}$$

- Case (4-iv): $\mathbf{a}_3^\perp \in \mathfrak{IV},\ \mathbf{a}_2 \in \mathfrak{II},\ -\mathbf{a}_2(1) > \mathbf{a}_3(1)$,

$$\boldsymbol{E}(\mathbf{x}) = \begin{cases} \xi(-\mathbf{k}\cdot(\mathbf{a}_1 + \mathbf{a}_2))\boldsymbol{E}(\mathbf{x} + \mathbf{a}_1 + \mathbf{a}_2), & \text{if } \mathbf{x} \in \mathrm{I} \\ \xi(-\mathbf{k}\cdot\mathbf{a}_2)\boldsymbol{E}(\mathbf{x} + \mathbf{a}_2), & \text{if } \mathbf{x} \in \mathrm{II} \\ \xi(\mathbf{k}\cdot\mathbf{a}_1)\boldsymbol{E}(\mathbf{x} - \mathbf{a}_1), & \text{if } \mathbf{x} \in \mathrm{III} \\ \boldsymbol{E}(\mathbf{x}), & \text{if } \mathbf{x} \in \mathrm{IV}. \end{cases} \tag{SM2.16}$$

In summary, the sixteen BCs (SM2.1)–(SM2.16) can be recast into

$$\boldsymbol{E}(\mathbf{x}) = \begin{cases} \xi(-\mathbf{k}\cdot\mathbf{t}_1)\boldsymbol{E}(\mathbf{x}+\mathbf{t}_1), & \text{if } \mathbf{x} \in \mathrm{I} \\ \xi(-\mathbf{k}\cdot\mathbf{t}_2)\boldsymbol{E}(\mathbf{x}+\mathbf{t}_2), & \text{if } \mathbf{x} \in \mathrm{II} \\ \xi(-\mathbf{k}\cdot\mathbf{t}_3)\boldsymbol{E}(\mathbf{x}+\mathbf{t}_3), & \text{if } \mathbf{x} \in \mathrm{III} \\ \xi(-\mathbf{k}\cdot\mathbf{t}_4)\boldsymbol{E}(\mathbf{x}+\mathbf{t}_4), & \text{if } \mathbf{x} \in \mathrm{IV}, \end{cases}$$

where definitions of $\{\mathbf{t}_i\}_{i=1}^4$ are self-evident in (SM2.1)–(SM2.16).

Similar to what is done in Part **III** of Sec. 4, we can express J_3 for (SM2.1)–(SM2.16) using $\{\mathbf{t}_i\}_{i=1}^4$ in a unified form. Define

$$m_2 = \mathbf{floor}\left(\frac{\overline{\mathrm{R}_9\mathrm{R}_1}}{\delta_x}\right),\ m_3 = \mathbf{floor}\left(\frac{\overline{\mathrm{R}_{10}\mathrm{R}_3}}{\delta_y}\right),\ m_4 = \mathbf{floor}\left(\frac{\overline{\mathrm{R}_{11}\mathrm{R}_2}}{\delta_x}\right), \tag{SM2.17}$$

then we have

$$J_3 = \begin{bmatrix} & I_{m_3} \otimes \begin{bmatrix} 0 & \xi(\mathbf{k}\cdot\mathbf{t}_3)I_{m_4} \\ \xi(\mathbf{k}\cdot\mathbf{t}_4)I_{n_1-m_4} & 0 \end{bmatrix} \\ I_{n_2-m_3} \otimes \begin{bmatrix} 0 & \xi(\mathbf{k}\cdot\mathbf{t}_2)I_{m_2} \\ \xi(\mathbf{k}\cdot\mathbf{t}_1)I_{n_1-m_2} & 0 \end{bmatrix} & \end{bmatrix}. \tag{SM2.18}$$

However, to derive the eigen-decomposition of J_3, a more useful form of J_3 should be used, *e.g.*, the one in the proof of Theorem SM2.2.

We also need to consider the BC (1.2) along the y-axis when $\mathbf{a}_2 \in \Im\Im$, which should differ from (3.4). Letting $\mathbf{x} = (x, b, 0) \in \mathbb{D}$, we have the BC (1.2) for different segments of $\mathrm{R}_3\mathrm{R}_2$ shown in, say, Figure SM2(c):

$$\boldsymbol{E}(\mathbf{x}) = \begin{cases} \xi(\mathbf{k}\cdot\mathbf{a}_2)\boldsymbol{E}(\mathcal{T}_{-\mathbf{a}_2}(\mathbf{x})), & \text{if } \mathbf{x} \in \mathrm{R}_3\mathrm{R}_8 \\ \xi(\mathbf{k}\cdot(\mathbf{a}_2+\mathbf{a}_1))\boldsymbol{E}(\mathcal{T}_{-\mathbf{a}_1-\mathbf{a}_2}(\mathbf{x})), & \text{if } \mathbf{x} \in \mathrm{R}_8\mathrm{R}_2. \end{cases}$$

Define

$$m_1 = \mathbf{floor}\left(\overline{\mathrm{R}_3\mathrm{R}_8}/\delta_x\right), \tag{SM2.19}$$

which is consistent with the one in Sec. 4. Then, depending on the quadrant in which $\mathbf{a}_2$ is located, J_2 in the discretized BC (4.5) has different form,

$$J_2 = \begin{cases} \begin{bmatrix} 0 & \xi(-\mathbf{k}\cdot\mathbf{a}_1)I_{m_1} \\ I_{n_1-m_1} & 0 \end{bmatrix} = K_1^{-m_1}, & \text{if } \mathbf{a}_2 \in \Im \\ \begin{bmatrix} 0 & I_{m_1} \\ \xi(\mathbf{k}\cdot\mathbf{a}_1)I_{n_1-m_1} & 0 \end{bmatrix} = K_1^{n_1-m_1}, & \text{if } \mathbf{a}_2 \in \Im\Im. \end{cases} \tag{SM2.20}$$

Consequently, we have a more general version of Theorem 5.6 as follows. Recall that in (2.2) $\mathbf{a}, \mathbf{b}, \mathbf{c}$ can also be expanded by $\mathbf{a}_1, \mathbf{a}_2, \mathbf{a}_3$ with expansion coefficients η_1, η_2, η_3 defined in (2.1).

THEOREM SM2.1. *K_2 in (4.7) is unitary. With X_i defined in (5.1), K_2 satisfies*

$$K_2(Y_{ij} \otimes X_i) = \xi(\theta_{\mathbf{b},i})\xi(j/n_2)(Y_{ij} \otimes X_i),\ i = 1, \cdots, n_1,\ j = 1, \cdots, n_2,$$

where

$$\theta_{\mathbf{b},i} = (\mathbf{k}\cdot\mathbf{b} - i\eta_1)/n_2, \quad \eta_1 = \begin{cases} m_1/n_1, & \text{if } \mathbf{a}_2 \in \mathfrak{I} \\ (m_1-n_1)/n_1, & \text{if } \mathbf{a}_2 \in \mathfrak{II}, \end{cases}$$

$$Y_{ij} = \left[1, \xi(\theta_{\mathbf{b},i})\xi\left(\frac{j}{n_2}\right), \cdots, \xi((n_2-1)\theta_{\mathbf{b},i})\xi\left(\frac{(n_2-1)j}{n_2}\right)\right]^\top. \tag{SM2.21}$$

Then we have a more general version of Theorem 5.10 as follows.

THEOREM SM2.2. *K_3 in (4.13) is unitary. With X_i and Y_{ij} defined in (5.1) and (SM2.21), respectively, K_3 satisfies*

$$K_3(Z_{ijk}\otimes Y_{ij}\otimes X_i) = \xi(\theta_{\mathbf{c},ij})\xi(k/n_3)(Z_{ijk}\otimes Y_{ij}\otimes X_i),$$

where

$$\theta_{\mathbf{c},ij} = [\mathbf{k}\cdot\mathbf{c} - \eta_3 j + (\eta_1\eta_3 - \eta_2)\, i]/n_3,$$
$$Z_{ijk} = \left[1, \xi(\theta_{\mathbf{c},ij})\xi\left(\frac{k}{n_3}\right), \cdots, \xi((n_3-1)\theta_{\mathbf{c},ij})\xi\left(\frac{(n_3-1)k}{n_3}\right)\right]^\top,$$

for $i = 1,\cdots,n_1,\ j = 1,\cdots,n_2,\ k = 1,\cdots,n_3$, with

$$\eta_1 = \begin{cases} m_1/n_1, & \text{if } \mathbf{a}_2 \in \mathfrak{I} \\ (m_1-n_1)/n_1, & \text{if } \mathbf{a}_2 \in \mathfrak{II}, \end{cases}$$

$$(\eta_2,\ \eta_3) = \begin{cases} (m_2/n_1,\ m_3/n_2), & \text{if } \mathbf{a}_3^\perp \in \mathfrak{I} \\ ((m_2-n_1)/n_1,\ m_3/n_2), & \text{if } \mathbf{a}_3^\perp \in \mathfrak{II} \\ ((m_4-n_1)/n_1,\ (m_3-n_2)/n_2), & \text{if } \mathbf{a}_3^\perp \in \mathfrak{III} \\ (m_4/n_1,\ (m_3-n_2)/n_2), & \text{if } \mathbf{a}_3^\perp \in \mathfrak{IV}. \end{cases}$$

Proof. Here we will just present the sketch of the proof, and the omitted details can be found in the proof of Theorem 5.10. For any of four categories mentioned above, say, j-th category, we have the following observations from Figure SM2, SM3, SM4 and SM5,

$$m_4 = \begin{cases} m_2 - m_1, & \text{Case } (j-i) \\ n_1 - m_1 + m_2, & \text{Case } (j-ii) \\ n_1 - m_1 + m_2, & \text{Case } (j-iii) \\ m_2 - m_1, & \text{Case } (j-iv). \end{cases} \tag{SM2.22}$$

Eq. (SM2.20) is also equivalent to

$$J_2 = \begin{cases} K_1^{-m_1} = \xi(-\mathbf{k}\cdot\mathbf{a}_1)K_1^{n_1-m_1}, & \text{if } \mathbf{a}_2 \in \mathfrak{I} \\ \xi(\mathbf{k}\cdot\mathbf{a}_1)K_1^{-m_1} = K_1^{n_1-m_1}, & \text{if } \mathbf{a}_2 \in \mathfrak{II}. \end{cases} \tag{SM2.23}$$

If $\mathbf{a}_3^\perp \in \mathfrak{I}$, considering (SM2.22) and (SM2.23), we have

$$\begin{aligned} J_3^* &= \begin{cases} \begin{bmatrix} 0 & I_{n_2-m_3}\otimes K_1^{m_2} \\ \xi(\mathbf{k}\cdot\mathbf{a}_2)I_{m_3}\otimes K_1^{m_2-m_1} & 0 \end{bmatrix}, & \text{if } \mathbf{a}_2 \in \mathfrak{I} \\ \begin{bmatrix} 0 & I_{n_2-m_3}\otimes K_1^{m_2} \\ \xi(\mathbf{k}\cdot\mathbf{a}_2)\xi(\mathbf{k}\cdot\mathbf{a}_1)I_{m_3}\otimes K_1^{m_2-m_1} & 0 \end{bmatrix}, & \text{if } \mathbf{a}_2 \in \mathfrak{II}, \end{cases} \\ &= (I_{n_2}\otimes K_1)^{m_2} K_2^{m_3}. \end{aligned}$$

If $\mathbf{a}_3^{\perp} \in \mathfrak{I}\mathfrak{I}$, considering (SM2.22) and (SM2.23), we have

$$J_3^* = \begin{cases} \begin{bmatrix} 0 & I_{n_2-m_3} \otimes K_1^{m_2-n_1} \\ \xi(\mathbf{k}\cdot\mathbf{a}_2)\xi(-\mathbf{k}\cdot\mathbf{a}_1) I_{m_3} \otimes K_1^{m_2-m_1} & 0 \end{bmatrix}, & \text{if } \mathbf{a}_2 \in \mathfrak{I} \\ \begin{bmatrix} 0 & I_{n_2-m_3} \otimes K_1^{m_2-n_1} \\ \xi(\mathbf{k}\cdot\mathbf{a}_2) I_{m_3} \otimes K_1^{m_2-m_1} & 0 \end{bmatrix}, & \text{if } \mathbf{a}_2 \in \mathfrak{I}\mathfrak{I}, \end{cases}$$
$$= \left(I_{n_2} \otimes K_1\right)^{m_2-n_1} K_2^{m_3}.$$

If $\mathbf{a}_3^{\perp} \in \mathfrak{I}\mathfrak{I}\mathfrak{I}$, considering (SM2.22) and (SM2.23), we have

$$J_3 = \begin{cases} \begin{bmatrix} 0 & I_{m_3} \otimes K_1^{n_1-m_4} \\ \xi(\mathbf{k}\cdot\mathbf{a}_2) I_{n_2-m_3} \otimes K_1^{n_1-m_1-m_4} & 0 \end{bmatrix}, & \text{if } \mathbf{a}_2 \in \mathfrak{I} \\ \begin{bmatrix} 0 & I_{m_3} \otimes K_1^{n_1-m_4} \\ \xi(\mathbf{k}\cdot\mathbf{a}_2)\xi(\mathbf{k}\cdot\mathbf{a}_1) I_{n_2-m_3} \otimes K_1^{n_1-m_1-m_4} & 0 \end{bmatrix}, & \text{if } \mathbf{a}_2 \in \mathfrak{I}\mathfrak{I}, \end{cases}$$
$$= \left(I_{n_2} \otimes K_1\right)^{n_1-m_4} K_2^{n_2-m_3}.$$

If $\mathbf{a}_3^{\perp} \in \mathfrak{I}\mathfrak{V}$, considering (SM2.22) and (SM2.23), we have

$$J_3 = \begin{cases} \begin{bmatrix} 0 & I_{m_3} \otimes K_1^{-m_4} \\ \xi(\mathbf{k}\cdot\mathbf{a}_2)\xi(-\mathbf{k}\cdot\mathbf{a}_1) I_{n_2-m_3} \otimes K_1^{n_1-m_1-m_4} & 0 \end{bmatrix}, & \text{if } \mathbf{a}_2 \in \mathfrak{I} \\ \begin{bmatrix} 0 & I_{m_3} \otimes K_1^{-m_4} \\ \xi(\mathbf{k}\cdot\mathbf{a}_2) I_{n_2-m_3} \otimes K_1^{n_1-m_1-m_4} & 0 \end{bmatrix}, & \text{if } \mathbf{a}_2 \in \mathfrak{I}\mathfrak{I}, \end{cases}$$
$$= \left(I_{n_2} \otimes K_1\right)^{-m_4} K_2^{n_2-m_3}.$$

□

SM3. J_2 and J_3 in other 13 Bravais lattices. As mentioned in Sec. 1, with necessary constraints imposed, the triclinic lattice can become other 13 Bravais lattices. Therefore, many results in other Bravais lattices can be directly inherited from those in the triclinic lattice.

Lattice translation vectors $\mathbf{a}_1, \mathbf{a}_2, \mathbf{a}_3$ of all 14 Bravais lattices can be found in [SM1]. The 3-by-3 matrix below is coordinates of $\mathbf{a}_1, \mathbf{a}_2, \mathbf{a}_3$ in the prior orthogonal coordinate system used in the crystallography database. $\widetilde{a}, \widetilde{b}, \widetilde{c}$ are lattice constants of the 3D physical cell. With the procedure to construct the orthogonal basis $\mathbf{a}, \mathbf{b}, \mathbf{c}$ of $\mathbf{a}_1, \mathbf{a}_2, \mathbf{a}_3$ and its important variation described in Sec. 2, we can similarly define the 3D working cell for other 13 Bravais lattices. For a specific Bravais lattice, we will present the matrix J_2 in (SM2.20) in terms of integer power of K_1 in (4.3). As for the matrix J_3 in (SM2.18), we either specify $J_3 = I_{n_1 n_2}$ or specify the subcategory in (SM2.1)–(SM2.16) to fix J_3. Recall that m_1 are defined in (SM2.19) and m_2, m_3, m_4 are defined in (SM2.17). However, if there are nothing special about $m_1, m_2, m_3, m_4, n_1, n_2$, we will not mention them below.

• Cubic system

(1) Primitive: $\widetilde{a} \begin{bmatrix} 1 & 0 & 0 \\ 0 & 1 & 0 \\ 0 & 0 & 1 \end{bmatrix}$, $J_2 = I_{n_1}$, $J_3 = I_{n_1 n_2}$.

(2) Face-Centered: $\frac{\widetilde{a}}{2} \begin{bmatrix} 1 & 0 & 1 \\ 1 & 1 & 0 \\ 0 & 1 & 1 \end{bmatrix}$, case (1-i),

$$m_1 = m_2 = n_1/2,\ m_3 = n_2/3,\ m_4 = 0,\ J_2 = K_1^{-m_1}.$$

(3) Body-Centered: $\frac{\widetilde{a}}{2}\begin{bmatrix}-1 & 1 & 1\\ 1 & -1 & 1\\ 1 & 1 & -1\end{bmatrix}$, case (3-iii),

$$m_1 = m_4 = 2n_1/3,\ m_2 = n_1/3,\ m_3 = n_2/2,\ J_2 = K_1^{m_2}.$$

• Hexagonal system: $\frac{1}{2}\begin{bmatrix}\widetilde{a} & \widetilde{a} & 0\\ -\sqrt{3}\widetilde{a} & \sqrt{3}\widetilde{a} & 0\\ 0 & 0 & 2\widetilde{c}\end{bmatrix}$, $m_1 = \frac{n_1}{2}$, $J_2 = K_1^{m_1}$, $J_3 = I_{n_1 n_2}$.

• Rhombohedral system: $\begin{bmatrix}\widetilde{a}/2 & 0 & -\widetilde{a}/2\\ -\sqrt{3}\widetilde{a}/6 & \widetilde{a}/\sqrt{3} & -\sqrt{3}\widetilde{a}/6\\ \widetilde{c}/3 & \widetilde{c}/3 & \widetilde{c}/3\end{bmatrix}$,

(1) if $\sqrt{2}\widetilde{c} < \sqrt{3}\widetilde{a}$, then case (3-iii), $m_1 = m_4 \geq n_1/2$, $J_2 = K_1^{n_1 - m_1}$.
(2) if $\sqrt{2}\widetilde{c} > \sqrt{3}\widetilde{a}$, then case (1-i), $m_1 = m_2$, $m_4 = 0$, $J_2 = K_1^{-m_1}$.

• Tetragonal system

(1) Primitive: $\begin{bmatrix}\widetilde{a} & 0 & 0\\ 0 & \widetilde{a} & 0\\ 0 & 0 & \widetilde{c}\end{bmatrix}$, $J_2 = I_{n_1}$, $J_3 = I_{n_1 n_2}$.

(2) Body-Centered: $\frac{1}{2}\begin{bmatrix}-\widetilde{a} & \widetilde{a} & \widetilde{a}\\ \widetilde{a} & -\widetilde{a} & \widetilde{a}\\ \widetilde{c} & \widetilde{c} & -\widetilde{c}\end{bmatrix}$, with $\widetilde{a} < \widetilde{c}$,

- **(a)** if $\widetilde{c} \leq \sqrt{2}\widetilde{a}$, then case (3-iii), $m_1 = 2(n_1 - m_4)$, $J_2 = K_1^{n_1 - m_1}$.
- **(b)** if $\widetilde{c} > \sqrt{2}\widetilde{a}$, then case (3-i), $n_1 - m_1 = 2m_4$, $J_2 = K_1^{-m_1}$.

• Orthorhombic system

(1) Primitive: $\begin{bmatrix}\widetilde{a} & 0 & 0\\ 0 & \widetilde{b} & 0\\ 0 & 0 & \widetilde{c}\end{bmatrix}$, $J_2 = I_{n_1}$, $J_3 = I_{n_1 n_2}$.

(2) A-Base-Centered: $\frac{1}{2}\begin{bmatrix}2\widetilde{a} & 0 & 0\\ 0 & \widetilde{b} & \widetilde{b}\\ 0 & -\widetilde{c} & \widetilde{c}\end{bmatrix}$, with $\widetilde{b} < \widetilde{c}$, $J_2 = K_1^{n_1 - m_1}$, $J_3 = I_{n_1 n_2}$.

(3) C-Base-Centered: $\frac{1}{2}\begin{bmatrix}\widetilde{a} & \widetilde{a} & 0\\ -\widetilde{b} & \widetilde{b} & 0\\ 0 & 0 & 2\widetilde{c}\end{bmatrix}$, with $\widetilde{a} < \widetilde{b}$, $J_2 = K_1^{n_1 - m_1}$, $J_3 = I_{n_1 n_2}$.

(4) Face-Centered: $\frac{1}{2}\begin{bmatrix}0 & \widetilde{a} & \widetilde{a}\\ \widetilde{b} & 0 & \widetilde{b}\\ \widetilde{c} & \widetilde{c} & 0\end{bmatrix}$, with $\widetilde{a} < \widetilde{b} < \widetilde{c}$, case (1-ii), $J_2 = K_1^{-m_1}$.

(5) Body-Centered: $\frac{1}{2}\begin{bmatrix}-\widetilde{a} & \widetilde{a} & \widetilde{a}\\ \widetilde{b} & -\widetilde{b} & \widetilde{b}\\ \widetilde{c} & \widetilde{c} & -\widetilde{c}\end{bmatrix}$, with $\widetilde{a} < \widetilde{b} < \widetilde{c}$,

- **(a)** if $\widetilde{c}^2 \geq \widetilde{a}^2 + \widetilde{b}^2$, then case (3-i), $J_2 = K_1^{-m_1}$.
- **(b)** if $\widetilde{c}^2 < \widetilde{a}^2 + \widetilde{b}^2$, then case (3-iii), $J_2 = K_1^{n_1 - m_1}$.

• Monoclinic system

(1) Primitive: $\begin{bmatrix}\widetilde{a} & 0 & \widetilde{c}\cos\phi_3\\ 0 & \widetilde{b} & 0\\ 0 & 0 & \widetilde{c}\sin\phi_3\end{bmatrix}$, with $\widetilde{a} < \widetilde{c}$, $\phi_3 \neq \pi/2$,

- **(a)** if $\phi_3 < \pi/2$, then $J_2 = K_1^{-m_1}$, $J_3 = I_{n_1 n_2}$.
- **(b)** if $\phi_3 > \pi/2$, then $J_2 = K_1^{n_1 - m_1}$, $J_3 = I_{n_1 n_2}$.

(2) A-Base-Centered: $\begin{bmatrix} \widetilde{a}/2 & \widetilde{a}/2 & \widetilde{c}\cos\gamma \\ -\widetilde{b}/2 & \widetilde{b}/2 & 0 \\ 0 & 0 & \widetilde{c}\sin\gamma \end{bmatrix}$, with $\gamma \neq \pi/2$, which is almost the same as the triclinic lattice.

REFERENCES

[SM1] *Crystal systems and lattices.* http://aflowlib.duke.edu/users/egossett/lattice/lattice.html.